USE OF AN EXPERIMENTAL TEST RIG TO STUDY THE IMPACT OF DRILLING PARAMETERS AND SIDE LOADS IN THE SIDE CUTTING TENDENCY OF A PDC BIT IN A HORIZONTAL SET UP

A Thesis

by

ANDRESSA ALVES GONCALVES

Submitted to the Office of Graduate and Professional Studies of
Texas A&M University
in partial fulfillment of the requirements for the degree of

MASTER OF SCIENCE

Chair of Committee,	Samuel Noynaert
Committee Members,	Jerome Schubert
	Alan Palazzolo
Head of Department,	A. Daniel Hill

December 2016

Major Subject: Petroleum Engineering

ABSTRACT

The demand for oil has increased considerably since its first discovery. Consequently, all of the reservoirs that were easy to access and/or explore have already been discovered. To overcome this challenge, the industry had to find a way to find new wells to explore, wells that were previously judged as non-economical, due to either their location or low porosity/permeability. For those reasons, the industry turned to directional wells, facilitated by the advances in technology. An important part of building a successful directional well is correctly predicting the well path. The objective of the present study is to analyze the influence of WOB, ROP, RPM and side load on the steerability of a PDC bit, bringing the work done by Ernst, Pastusek and Lutes (2007) to a horizontal set up and analyzing the response of MSE while sidecutting. Findings suggest how much of an influence the drilling parameters have on steering the bit, and the knowledge of how they affect the set up used during drilling can be a fundamental tool when creating a well path.

The tests were conducted on a horizontal test rig, built by the Mechanical Engineering Department at Texas A&M University, using 8 ksi average compressive strength samples. During the tests, modifications had to be made to the rig in order to accommodate the demands of a petroleum drilling operation. An innovative system was installed to measure shaft deflection through a HD Webcam, turning distance in the pixels from the images captured into real life

distance. Through that system it was possible to back calculate the side load being applied to the system, controlling it in real time.

The results showed that two parameters were the most influential on the sidecutting angle of a PDC bit: side load and RPM. Side load was even more significant for lower values, where an increase is much more abrupt. ROP is also expected to have a smaller influence, and it was observed for the sample with the highest RPM. MSE showed an expected response, being opposite to the side load. The results observed were very similar to the ones found by Ernst, Pastusek and Lutes (2007), thus being possible to conclude that when drilling a vertical well, the bit will respond in a similar manner to the changes in drilling parameters as it would in a vertical well.

DEDICATION

This work is dedicated to my wonderful husband Jonathan. You have stuck by my side throughout it all, enduring meltdowns, wiping away tears, telling me I could do it and believing in me even when I did not believed in myself. You are the best partner I could ever have asked for and I am very blessed and thankful to have found you. You are my rock, my prince charming and my best friend and I love you unconditionally. Always.

ACKNOWLEDGEMENTS

I would like to thank my committee chair, Dr. Noynaert, and my committee members, Dr. Schubert, Dr. Palazzolo, for their guidance and support throughout the course of this research.

I also need to thank the Brazilian Federal Agency for the Support and Evaluation of Graduate Education (CAPES) Foundation, Ministry of Education of Brazil, Brasilia – DF, Zip Code 70.040-020 for providing the funding for my time at Texas A&M University under grant 88888.076084/2013-00.

A special thanks to Erwin “Tom” Thomas, for all his support. I would also like to extend thanks to Natieli Lima, Rafael Oliveira, Kyle Paradis, Enrique Losoya, Jason Jackson, Henry Serry and Michael Martin for the much needed assistance.

Finally, I need to thank my family, the ones back in Brazil for their love and support, even from halfway across the word. I know it was not easy to worry and be apart, but they always encouraged me to follow my dreams and better myself. And the ones I found here, for taking me in from day one as a daughter and loving and supporting me ever since.

NOMENCLATURE

α	Angle of Hole Inclination
Φ	Angle of Inclination of Force on Bit
δ_e	Deflection as predicted by Euler's equation
δ_s	Deflection caused exclusively by side cutting
δ_t	Total deflection
δ_{eb}	Deflection predicted by Euler's equation at the bit
δ_{ec}	Deflection predicted by Euler's equation at the camera
δ_{mb}	Deflection measured at the bit
δ_{mc}	Deflection measured at the camera
δ_{sb}	Deflection due to sidecutting at the bit
δ_{sc}	Deflection due to sidecutting at the camera
θ_e	Maximum angle caused by shaft deflection as predicted by Euler
θ_o	Overall angle
θ_s	Angle due exclusively to sidecutting
BHA	Bottom Hole Assembly
BS	Bit Steerability

CAPES	Brazilian Federal Agency for the Support and Evaluation of Graduate Education
D	Bit Diameter
DLS	Dog Leg Severity
DOC	Depth of Cut
E	Young's Modulus of shaft
F	Force
HWDP	High Weight Drill Pipe
I	Moment of Inertia
KOP	Kick Off Point
l	Distance from the shaft origin
L	Total length of the shaft
MSE	Mechanical Specific Energy
NPT	Nonproductive Time
PDC	Polycrystalline Diamond Compact
PDM	Positive-Displacement Motors
r	Internal Radius of the Shaft
R	External Radius of the Shaft
ROP	Rate of Penetration

RPM	Rotation per Minute
RSS	Rotary Steerable
TOB	Torque on Bit
WOB	Weight on Bit

TABLE OF CONTENTS

Page

LIST OF FIGURES

Page

LIST OF TABLES

Page

1 INTRODUCTION

Millheim (1977) defined hole curvature to be when there is a change on inclination and azimuth throughout the path of a well. That change can result in a directional well. When the inclination angle is between 80 and 100 degrees, the well is then called a horizontal well. According to Millheim (1977) some of the most important characteristics influencing in the hole curvature are oscillation, weight on bit (WOB), formation hardness, jetting and downhole motors. Walker (1986) also mentions borehole geometry, formation and operating conditions and equipment as some of the factors that affect the hole angle and direction.

Directional wells are nothing new to the oil business, with the first recorded well to be drilled purposely directionally to reach an objective being in the early 1930s in California, where a rig located on land was used to drill a well under the sea bed. In 1934, a directional well was used to relieve a blow out on the Conroe Field, in East Texas, exploring further applications of directional wells. By the end of World War II, different fields had been made economically viable due to drilling multiple directional wells from a single drilling rig (Inglis 1987).

Directional drilling has become more popular (**Figure 1**) with the advances made in technology and with the increasing demand to produce more oil that led to the exploration of reserves that were once thought as impossible to produce from and/or uneconomical. With this increase in popularity, the productivity in thinner reservoirs and the maximization of production were able to be achieved,

however the following challenges started to present themselves: optimizing hole quality, tool face control, vibrations (bit and BHA) and build rate or hole curvature prediction (Pastusek, Brackin and Lutes 2005).

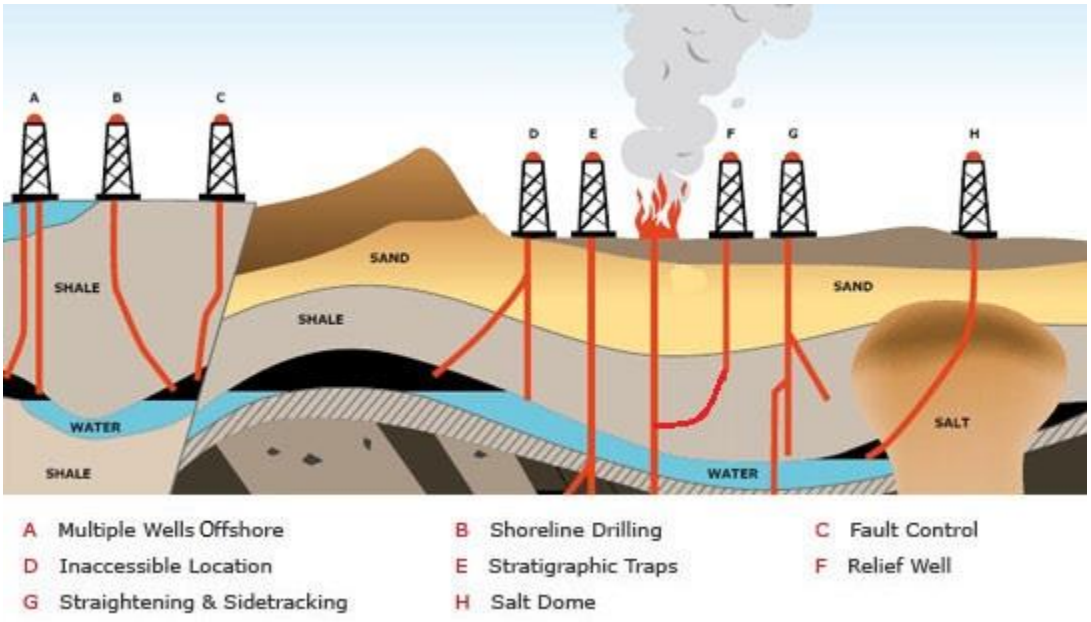

Figure 1 - Some of the current uses of directional wells (Kakogianis and Schroder 2011).

The targets are reached by having build up, hold and drop off sections, on a vertical plane, and/or by having a change in azimuth in the horizontal plane, which will guide the well until it reaches the desired location (**Figure 2**).

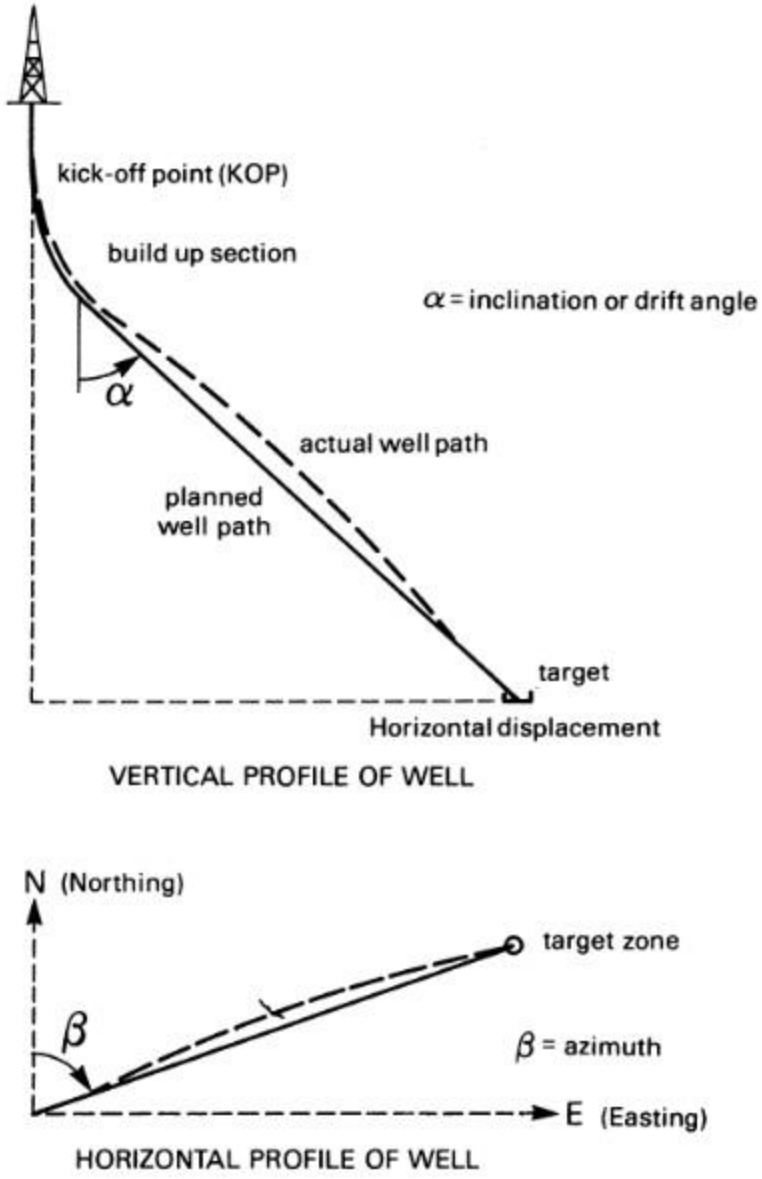

Figure 2 - Detailed view of the vertical and horizontal plans of a directional well (Inglis 1987).

1.1 Directional Drilling Techniques

The heterogeneity of the formations being drilled can influence the deviation of the drill string. Steeper dipping formations will keep the bit drilling

parallel to the bedding planes, whereas in less steeply dipping formations the bit and the bedding planes will be at a right angle (Inglis 1987).

Components of the BHA such as drill collars and heavy weight drill pipe (HWDP) can be used to provide more WOB. Generally, increasing WOB will build angle, while a decrease in WOB will drop angle. This is not the best way to cause drops because a reduction in WOB can result in less depth of cut (DOC), which can cause more whirl and thus bit damage (Dupriest et al. 2010).

Stabilizer positioning has also been known to help with build/drop angle and Walker (1986) predicted how the placement would affect the drill string (if all the other drilling conditions are constant) as illustrated by **Figure 3**. Stabilizers placed further away from the bit result in drop angle, while placing a stabilizer closer to the bit would help maintain or even build angle.

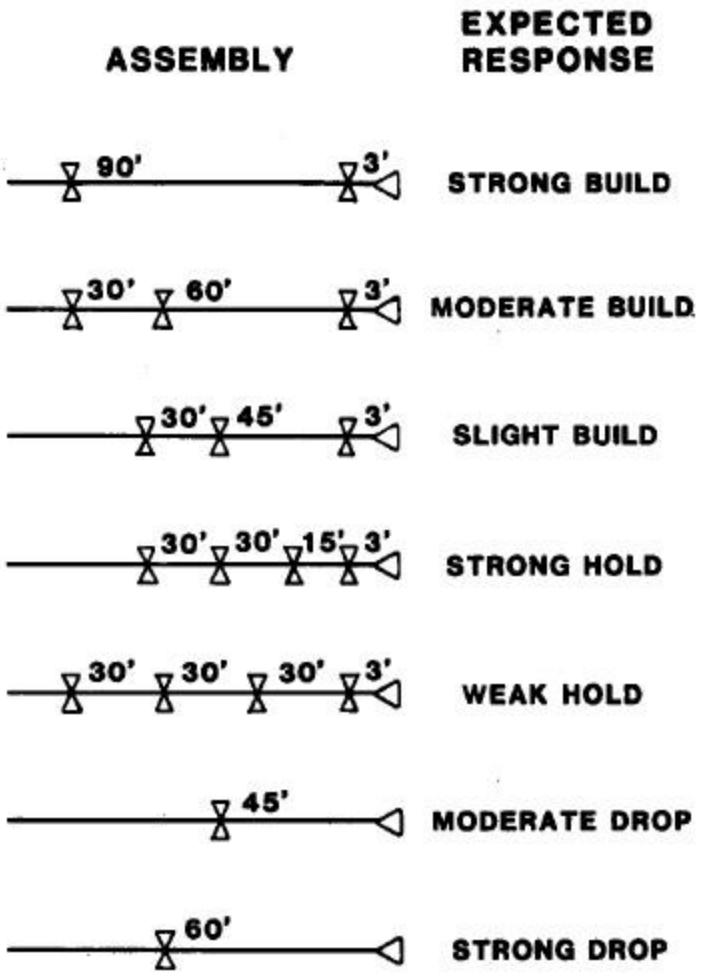

Figure 3 - Stabilizer placement and its expected influence on the build/drop angle of a drill string (Walker 1986).

The interaction of WOB, torque and RPM in affecting the well trajectory are well known to the industry as the pendulum effect, where stabilizer placement and point of first hole contact (**Figure 4**) can cause the hole to return to the vertical position or to build/drop angle (Walker 1986).

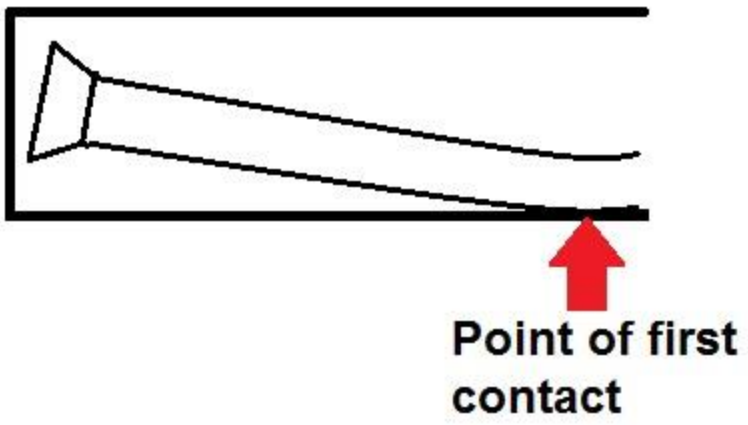

Figure 4 - Schematic showing the first point of contact between the drill string and the wellbore.

1.2 Directional Drilling Technologies

The most commonly technologies for directional drilling in use today are Positive-Displacement Motors (PDM) (or mud motors) and Rotary Steerable Systems (RSS).

PDMs typically contain a bend near the bit to form a steerable motor that can be run in both sliding (bent sub is oriented so it can reach the inclination and azimuth changes, and only the drill bit rotates) and rotating (entire drill string rotates) drilling modes. PDMs consist of five basic components (**Figure 5**): dump valve, power assembly, connecting rod, bearing and drive shaft and bit sub. The power assembly is where the torque is generated and it is composed of a rotor and a stator (fixed in the housing), both with helical lobes. The rotor is activated by the flow of drilling fluid and the dump valve is in place to prevent fluid to enter the drill string. The connecting rod is what transmits rotational motion to the bit. (Mitchell and Miska 2010).

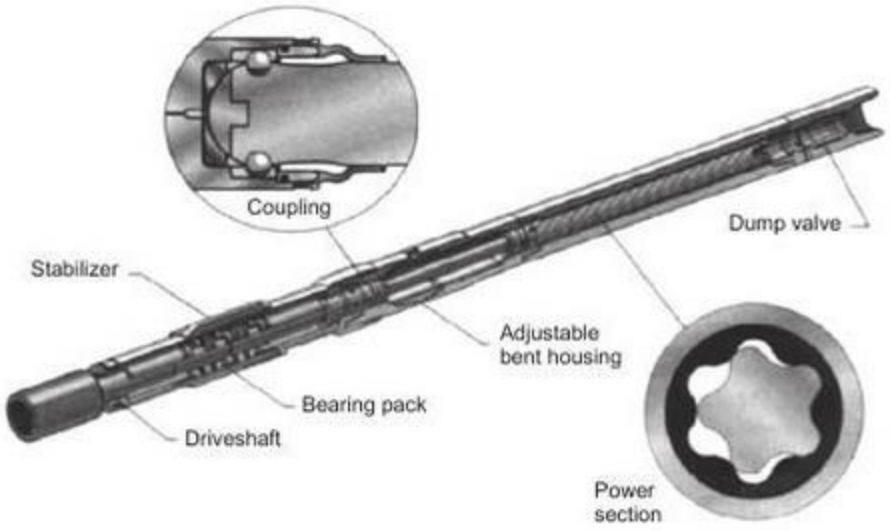

Figure 5 - Main components of a PDM attached to an adjustable bent housing (Mitchell and Miska 2010) *apud* (Underwood and Payne 1997).

With RSS, for the bit to be steered, there is no sliding required, and the directional changes can be done while the string is rotating. They can have configurations that are pure point-the-bit, pure push-the-bit, or a combination of both (**Figure 6**). For push-the-bit configurations a side load is applied to the bit through pads that do not rotate after they are pressed against the hole wall. They are more effective with short-gauge bits with active side cutting abilities. Point-the-bit configurations has a principle that is similar to PDMs, where a steering structure is tilted by a shaft to orient the direction of the drilling (inclination and azimuth). A hydraulic system allows the bit to be moved and pointed to the desired direction (Mitchell and Miska 2010).

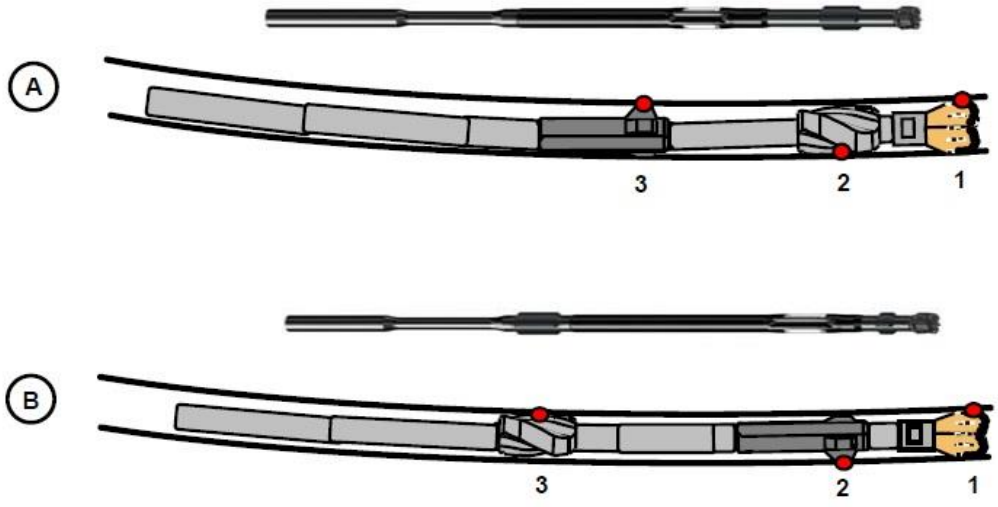

Figure 6 - Point-the-bit (A) and push-the-bit (B) configurations of a RSS (Jones, Sugiura and Barton 2008).

1.3 Bit Influence

The bit itself can influence the directional tendency of the well. The terms used to describe the bit's effect on the wellbore trajectory are the walk tendency (bit turn) and steerability. The walk tendency is the angle between the lateral force that was applied and the lateral displacement of the bit, perpendicularly to the axis of the bit, and is responsible for the azimuth changes of the bit. If the lateral displacement is on the left of the lateral force, the bit is said to have a left tendency, whereas if the displacement is on the right of the lateral force, the bit has a right tendency. If both the displacement and the force are on the same plane, the bit is neutral. PDC bits usually have left tendencies, while roller cone bits usually have right tendencies. The bit steerability (BS) is the capacity of the bit to deviate when

under lateral and axial forces, and it can be defined by the ratio between lateral and axial drillability.

The bit has three main parts that will interact with the formation, thus influencing on the directional behavior of the bit, which are the cutting structure (cutting profile and back rake angle), the active gauge (trimmers or cutters) and the passive gauge (gauge pad) (**Figure 7**) (Menand, Sellami and Simon 2003, Menand et al. 2002).

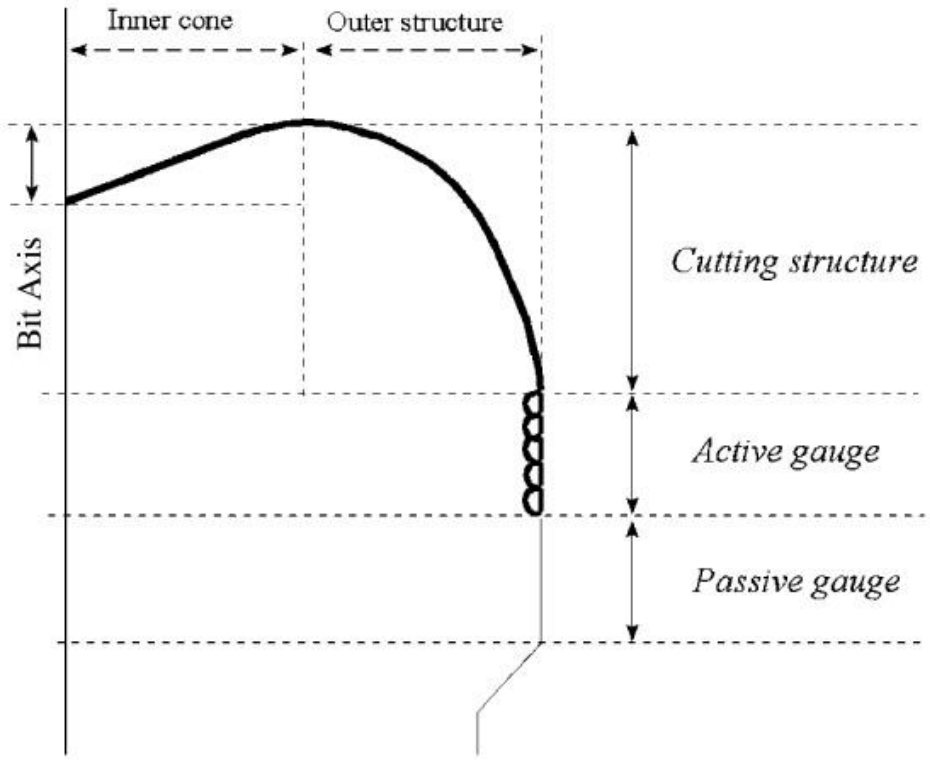

Figure 7 - Three main PDC bit parts that interact with the formation, influencing with the directional behavior of the bit after Menand et al. (2002)

1.3.1 Cutting Structure

Menand et al. (2002) found in their study that the cutting structure is dependent on the bit cutting profile, where the steerability of the bit is proportional to the flatness of the cutting profile of the bit. They also found a relationship between the heights of the inner cone and the outer structure. If the outer structure is higher than the inner cone, the bit will have a left tendency. If the inner cone is higher than the outer stricter, the bit will tend to the right. Finally, if they have the same sizes, the bit will be neutral.

For a back-rake angle analysis, there is a lot of controversy in the literature, however, in Menand, Sellami and Simon (2003) the authors state that the axial drillability is more affected than the lateral drillability by a change in back-rake angle and that its increase will also increase the BS.

1.3.2 Active Gauge

Menand, Sellami and Simon (2003) point out some conflicting studies done regarding the relationship between the number of gauge cutters and BS, but they conclude that BS will increase with the number of gauge cutters.

The authors also mention the gauge cutters provide two contact points with the formation: a cutting face and a frictional surface. The frictional surface is crucial in providing cutting ability to the bit, and the higher it is, less steerable the bit will be.

1.3.3 Passive Gauge

The gauge pad length selection is a critical design choice because short aggressive gauges will increase BS but can result in poor borehole quality. On the other hand, longer gauges will have lower steerability, but will provide better hole quality. When using a RSS, usually a point-the-bit configuration will use a long gauge bit, while a push-the-bit configuration will use a short gauge bit.

1.4 Research Objectives

Whenever there is a low quality well, or even a decrease in the efficiency of the drilling, it can end up in nonproductive time (NPT) due to workover or sidetracking, per example. This becomes more evident in high cost wells, which is the case in directional drilling. Those types of wells require more technology and are often done in sensitive/extreme environments (offshore, for example), which are very costly. For that reason, those projects are carefully evaluated and every factor is studied to make sure the drilling process will be the most efficient. And in many cases, that planning is key to making the well economically viable, which is why knowing how every factor will affect the well path becomes even more crucial in a directional well.

The present work is an effort to analyze WOB, ROP, RPM and lateral loads and how they will affect the steerability of a PDC bit, taking the work done by Ernst, Pastusek and Lutes (2007) and furthering to a horizontal scenario, evaluating the differences and similarities between vertical and horizontal

scenarios . Another point of the research is to analyze MSE and how it responds while sidecutting.

2 LITERATURE REVIEW

2.1 Directional Drilling Tendencies as a Function of the BHA

Lubinski and Woods (1953) published a study combining an analysis of the forces acting on the bit and the property of the formations to be drilled to relate the change of the angle of inclination of the well path to the factors influencing them. Their work was the first of the kind and to this day it is still largely cited. What they defined as “point of tangency” has been defined on the present work as point of first contact. When there is no WOB, the forces acting on the bit are resultant of the portion of the drillstring between the point of tangency and the bit and they tend to bring the well path to the vertical. When there is WOB applied, it will tend to bring the well path away from the vertical. The resultant of these forces will cause the angle to increase, decrease or be maintained. With those data they derived graphs showing that relationship for different examples, as demonstrated by **Figure 8**.

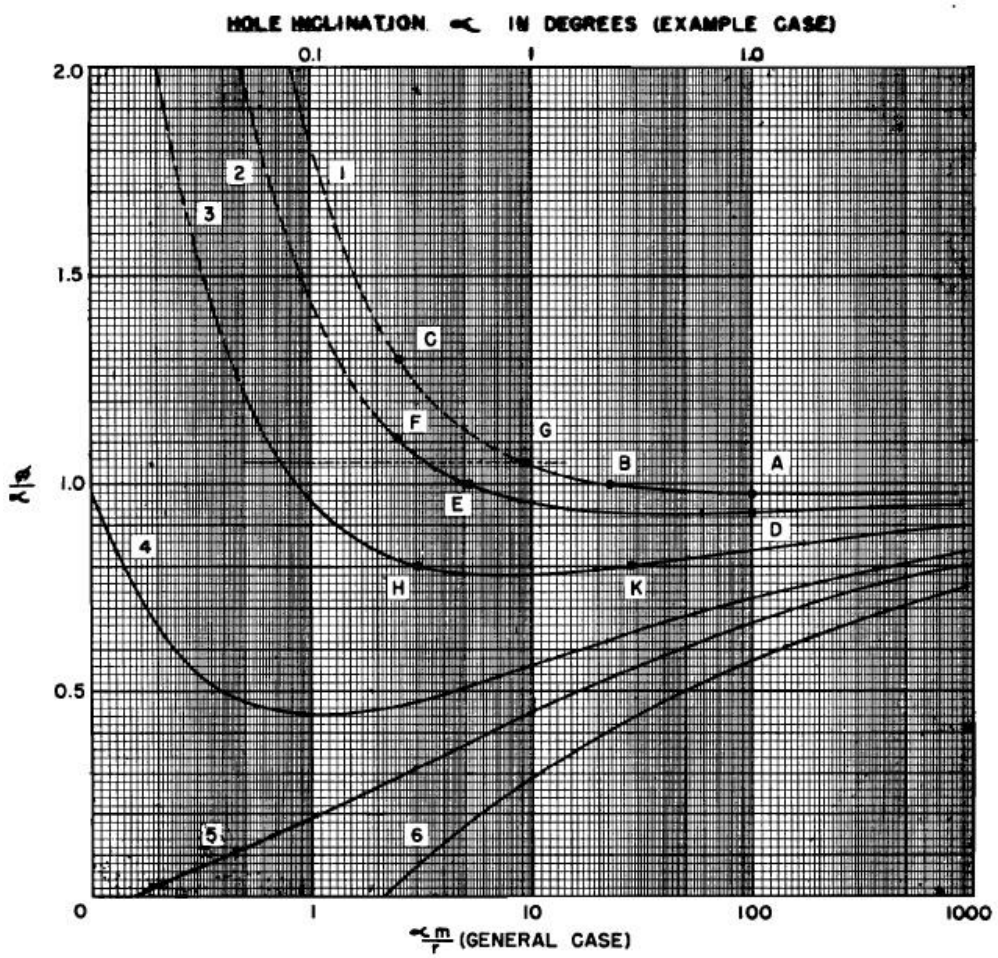

Figure 8 - Relationship between the ratio of Angle Φ of Inclination of the force on bit over Angle α of Hole Inclination (Lubinski and Woods 1953).

They developed specific charts for different BHA's and hole sizes and each line on the graph would correspond to a different WOB. If $\frac{\Phi}{\alpha}$ is less than 1, there will be a drop in the angle, whereas if the ratio is bigger than 1 there will be an increase in the angle. If the ratio equals 1, than there is no change to the inclination of the hole. They found that the use of large drill collars helped to maintain the well path with no deviations. Larger collars also allowed the use of more WOB

without a change in hole inclination. They also found that the BHA would have a tendency to reach an equilibrium, that is after the inclination reached the direction of the formation, the drilling would continue to be in that angle (considering all other conditions to be the same).

Millheim, Gubler and Zaremba (1978) developed a computer program, based on finite element, to calculate the 3D forces and dislocation in a BHA that is under axial loads. Their program can be used to either plan the BHA to be used in the well or in a post analysis approach. For post analysis, a large amount of high frequency data is crucial: measured depth, inclination, and direction, WOB, RPM, ROP, lithology, bit details, BHA configuration and dimensions, tool facing and inclination and direction. Then an initial plot is done with measured depth on the ordinate and the other parameters across the abscissa, with a mark to signalize change in bit and/or BHA. Other information such as casing size and depth, mud motor run, washouts and sidetracks and points where the tools got stuck can also be inputted as keynotes. The authors stated that the advantage of having a high volume of data is the ability to explain the trajectory changes generated by faults, formation effects, bit walk and contradictory behavior of BHA. The 3D program used for analyzing the BHA behavior used the finite element model, a method that divided the BHA into constant discrete elements of the cross sectional geometry. For each element, a matrix that related force to displacement is calculated. Whenever an iteration is completed without significant changes in the displacement, the solution is completed. Three movement directions were

possible: the axial force caused the bit to drill ahead, whereas side force caused the bit to drill sideways (positive side force was equivalent to a build tendency, while a negative force was a dropping tendency). Lower angle inclinations had a horizontal component significant enough to cause the bit to deflect. The initial boundary condition was that both the bit and stabilizer would not be able to displace further than the diameter of the hole. They used the post-analysis to further refine the method and found that the hole curvature above the bit should be used instead of a constant inclination model. This study was extremely important in showing the necessities of the industry, and relating BHA analysis to a post-analysis method. That combination can still be applied in training personnel even though a lot of better studies have come after that.

Jogi, Burgess and Bowling (1986) study showed how a 3D static analysis of the BHA can help predicting the directional inclination of rotary assemblies. The model proved to be very useful, especially in unknown situations, with an unused BHA configuration. In addition, the 3D aspect allowed the geometry of the wellbore to be considered and also enables the downhole torque to be modeled. The fact that the model has an analytical solution instead of a numerical one (finite element) made this model faster and therefore more suitable for use on a rig site. They were able to predict three important features: side force both at the bit and at the stabilizers (which is used to qualitatively find the build/drop tendencies of the BHA), the deformation of the BHA (which is used to monitor the collars, if they are under excessive stress or if they are in contact with the borehole), and the

stability of the BHA (which predicts the build/drop and turn rates). Their data came from seventeen bit runs in three wells in the gulf coast. They found that out of the 17 BHA's, 13 seemed to reach equilibrium (stable tendency of the BHA) in an average of 100-400 ft and in nine of those cases the model predicted the equilibrium behavior with an accuracy within 0.1°/100 ft. For seven BHA's the predicted equilibrium was within 0.4°/100 ft, however they observed that all of those wellbores were enlarged. For one particular assembly (the only one ran with near-bit stabilizer), their result of 0.6°/100 ft was significantly greater, but they found that having a different input for the stabilizer in the model would have gotten the results to the 0.1°/100 ft mark as well. They also observed that poor predictions were made during the runs were the ROP was lower than 40ft/hr, but they managed to correct them by entering a hole overgauge into the model. Their model is very useful in situations where the BHA is new and untested and the fact that it can be used in a rig site is one of the biggest advantages of the model. However their predictions can be easily matched by a driller with a lot of experience in the area to be drilled or with the BHA in use.

Jones, Sugiura and Barton (2008) conducted tests in wells with different bit features and RSS configuration. The drill bit tests were done in a controlled environment, enabling the relationship between gauge geometry and configuration to be studied without a change in the cutting structure. The RSS they used was able to run both point-the-bit and push-the-bit configurations. For the former a stabilizer was placed near the bit and used as a mean to tilt the bit

and direct it, and for the latter the steering unit was the one that pushed the bit to the desired direction. They were able to monitor near-bit caliper, stick-slip and vibration, using four different gauge configurations to determine variation in stability and steerability (the cutting structure was the same, thus the side cutting capability was the same, leaving the variation in stability and steerability as the variables affected by different gauge configurations). They were: active gauge, dual action gauge, circumferential gauge and tapered gauge (**Figure 9**).

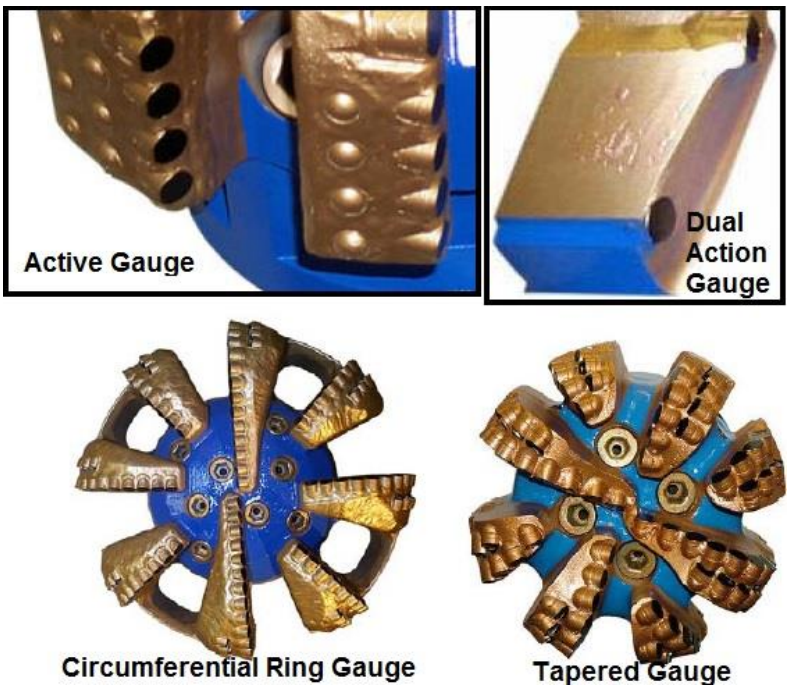

Figure 9 - Different types of gauges used on the study (after Jones, Sugiura and Barton (2008).

They found that the design of the bit for each RSS should be customized, matching the appropriate bit for the desired application which primarily depends

on the RSS driving mechanism and rock type. The optimal selection results in the best drillability, stability, steerability and borehole quality. Their work, while valid, does not provide a systematic method to predict the best gauge structure to the RSS drill bit. Their conclusions can be used as a start, but they state that every case has to be closely studied depending on the formation to be drilled. This approach is impractical when considering a real life situation where time is highly valued. That study might be done in an exploration well, but it is not realistic on a day-to-day drilling operation.

Menand et al. (2012) studied the differences between the push-the-bit and the point-the-bit methods of RSS, analyzing the influence of both side force and bit tilt in deviation. Their test consisted of using a full-scale drill bench (**Figure 10**) to drill a rock sample at atmospheric pressure while applying a side force and shaft tilt.

Figure 10 - Full-scale drilling bench used to conduct the experiments (Menand et al. 2012).

The tests started with a vertical phase and then proceeded with applying the force related to the configuration necessary to conduct the desired test (push-the-bit, point-the-bit or a hybrid) when the gauges were completely into the rock. With the push-the-bit configuration only a side force is applied through an electric jack, while with the point-the-bit configuration the force was applied to the shaft holding the sample using a hydraulic jack, and the hybrid configuration allows a shaft tilt control while applying a side force onto the bit. Approximately 100 tests were conducted in both soft and hard sandstone and the ROP, WOB, Torque on

bit (TOB) and RPM were measured, while hole deviation and bit tilt were measured after the holes had been drilled. They found that, regardless of the configuration, bits with the same cutting structure would point in the same direction at the beginning of the deviation. After that, tilt made the bit deviate to one side even though side force on the bit pointed to the opposite direction. A bit with high BS (steerable) will not be highly influenced by bit tilt and will follow the side force deviation, which would also happen with a bit that has a strong side cutting ability. While a bit with low BS will follow the tilt deviation, pattern that will also be followed by bits with longer or less aggressive gauges. Their work is very interesting and their findings are very useful when selecting a bit. The one detail that would elevate even more their study is doing the tests under well conditions. Verifying if the same trends are true in a field study would make their conclusions even more relevant to the industry.

2.2 Directional Drilling Tendencies as a Function of the Rock-Bit Interactions

Millheim and Warren (1978) conducted a study with a full scale drilling device that measured the side cutting characteristics of the bit. Variables like RPM, ROP, WOB, side load and bit mechanics were maintained constant throughout the experiments. The WOB is generated by a hydraulic system, which together with a ramp generator controls the ROP. The RPM is also controlled by hydraulics. In order to test the side forces the rock was put in a roller system that

enabled it to move horizontally. Another hydraulic cylinder applied the force to the rock, in the same direction of its freedom of movement. In addition, a drill collar and two restraining bushings were installed around the drill string to prevent its bending. The tests were done in samples from Bedford Limestone and Carthage Marble. The bits were tested by drilling a 6” hole with a constant ROP. During that process the RPM was adjusted to the value to be used. When that depth was reached, the side load was applied and the drilling continued until 4’, with all the parameters constant. In the Carthage marble they observed that the rate of the side cutting would decrease until reaching a constant point of dislocation. They also noted a significant change in the rate of side cutting with a small change in the side force, a tendency that was observed in the Bedford limestone as well. Another observation for the Bedford limestone was the effect that different ROPs had on the displacement rate. In general they were able to observe that the side force and the displacement rates were directly related, while ROP and the displacement rate were inversely related. Their study was a clear beginning of work addressing the needs of a changing drilling industry and when combined with a finite element BHA modeling would be very useful in helping predicting the well path, leaving a lot to be explored in the following years.

Cheatham Jr. and Ho (1981) created a model considering the assumpions that three constants describing rock drillability would affect the drilling rates in three orthogonal directions (if all other factors are constant) and two constants would affect the drilling rate for the bit along its axis and in the radial direction.

When all constants were used in their equation, the result was a relationship which described result of the bit drilling an isotropic rock. Those constants allowed them to develop a linear mathematical model that would predict the drilling direction when drilling an anisotropic rock. Their equations related the drilling rates to the force on the bit, the bit drilling characteristics and the rock paramenters, which in turn related the directional bit tendency to both rock and bit characteristics. They were able to prove, from numerical examples, that the interactions between the bit and the anisotropic rock can cause the bit to deviate where there is no force component present. However, being a numerical model, its use on a rig site is likely out of question due to the time consuming resolution it provides. Also, there was no mention to an experimental verification of the model to further validate their results.

Boualleg et al. (2006) and Boualleg et al. (2007) conducted tests of a drilling program on a full-scale drilling bench (**Figure 10**). Directional tests were also conducted in order to better understand the rock-bit and the bit-string interactions.

Their objective was to minimize the tortuosity when drilling a well, focusing on the formation anisotropy (considering that most studies have been done only on isotropic rocks, leaving the anisotropic rocks lacking more in depth research studies), especially interbedded and laminated rocks. Their cutter-rock interaction model calculates the specific energy considering laminated failure, which takes into account 3D variation of dip orientation. Their bit-rock interaction model then

used the cutter-rock model to calculate the force on each cutter and added them to determine the forces on the bit. For interbedded rocks, the model is capable of adapting the parameters according to the rock (soft or hard rock) through the radial position of each cutter to the interface. For laminated rock, where the specific energy varies more significantly with angular position, the model is able to calculate the formation dip relative to the cutting direction of each cutter. For the interbedded rocks the laboratory tests consisted of drilling different rocks (hard/soft and soft/hard) with inclined contact. They recorded lateral force, WOB, TOB and bending moments, as well as conducted measurements on the deviations on the borehole. The bit suffered two different types of lateral forces: anisotropic rock side force (caused by the fact that not all the cutters are acting on the same rock at the same time) and shaft side force (caused by the shaft tendency to bring the bit back to the vertical position after it deviates due to the change of rock – soft/hard). They observed that the deviation and the WOB were closely related. For the soft rock, it remained constant and on the revolution axis of the bit. In contrast, when drilling through the hard rock, it was observed that the WOB increased and became decentralized (not applied on the revolution axis of the bit), causing a bending moment. However, once all the cutters are in the hard rock, the WOB would go back to its previous state, leading to a conclusion that the side force effect is higher than the bending moment. Sequences with higher dip angles presented higher side forces and deviations, caused by the longer time drilling through the contact. Also, the use of different bits showed that the gauge

led to a higher up-down deviation, reduced perpendicular deviation, and better borehole quality. The laminated rocks used in the experimental laboratory tests were Tournemire shale, preserved to maintain its natural humidity and avoid changes in mechanical characteristics, with the dip angle varying from 5° to 85°. Initially, the ROP was accelerated to up to 0.018 ft/s and then maintained at that speed with a RPM of 1.42 rev/s. During the last step of the experiments, they observed an increase on the lateral force, proving that there is a side force, most likely due to the rock anisotropy (whether they are interbedded or laminated), and that the side force increased with the dip angle, varying from -20° to 45° around the down to up direction. They also conducted experiments applying a lateral force to the rock sample from down to up dip and from up to down dip as well. In the first case, the anisotropic side force helped the force applied, whereas in case two, it worked against it, indicating that the anisotropic side force could impact the directional behavior of the bit (**Figure 11**).

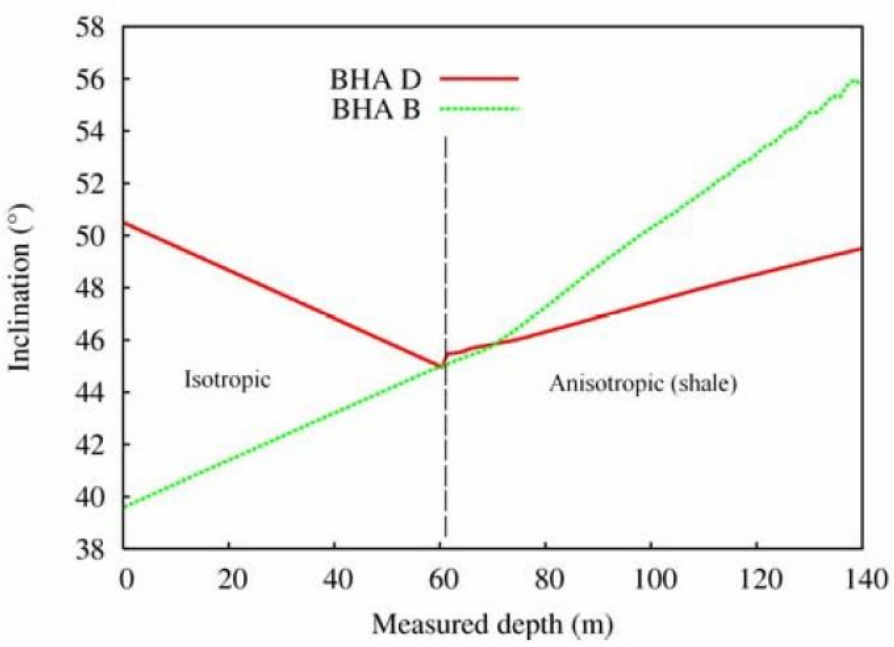

Figure 11 - Effect of anisotropy on build/drop rate, showing how much it can affect the directional drilling (Boualleg et al. 2006).

The main advantage of this model is the fact that it was developed for anisotropic rocks. That fact alone makes the model a lot more useful and applicable to real life scenarios. Using a test rig bench also helps the model to be verified under conditions closer to what is seen in downhole conditions, making their findings more valid.

Gerbaud, Menand and Sellami (2006) developed a cutter/rock interaction model that takes into consideration the presence of a build-up edge of crushed materials on the cutting face, and also the chamfer's shape and size, which affects ROP. Their objective was to increase cutting efficiency, bit steerability and ROP through decreasing mechanical specific energy (MSE). The authors use the total

force acting on the polycrystalline diamond compact (PDC) cutter as being the sum of the forces acting on the cutting face (where the authors incorporated the effects of the build-up edge of the crushed materials), the forces acting on the chamfer surface (where different mechanisms were used depending if the DOC was greater or lower than the chamfer height) and the forces acting on the back cutter surface (deformation done to the back of the cutter and the crushed material that find their way to the back of the cutter).**Figure 12** shows a schematics of the forces in action in a PDC cutter.

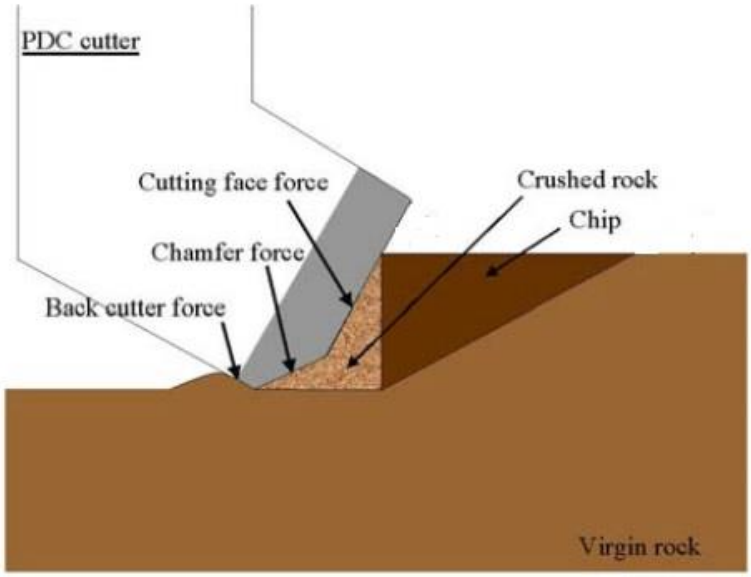

Figure 12 - Forces applied to the PDC cutter (after Gerbaud, Menand and Sellami (2006)).

They ran tests in a scale laboratory drilling tests in atmospheric conditions and in a drilling cell, at a constant speed and DOC, in sandstone and limestone.

Three different diameters of cutters were used. Then the forces in all 3 directions were recorded. They found that the build-up edge of crushed rock made it possible to increase the back rake angle to values greater than 20° (**Figure 13**) and that in small DOC the normal chamfer force can represent over 50% of the normal force (which is a well known fact and shows that the bit is being run inefficiently). Finally they found that the relief angle of the back cutter and the cutter force are inversely related. The success of their model was proved during a field test in Gabon, where a new bit was designed according to their principles and they were able to drill a slim hole project with a ROP 2.6 faster than the previous bit used.

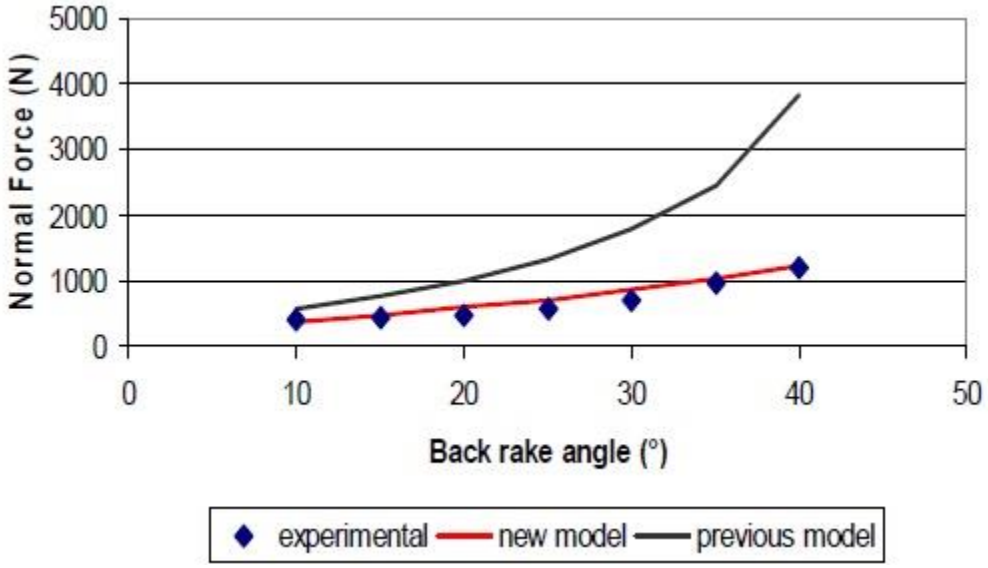

Figure 13 - Relationship between force caused by crushed materials and back rake angle (Gerbaud, Menand and Sellami 2006).

The innovations described generated benefits in terms of ROP, optimizing it by knowing which bit cutter would be better suited for that well's needs. Another benefit was in bit stability because the model provides a PDC bit with balanced radial force and bending moment. Finally, the estimation of the bit steerability and walk angle enables the prediction of how the bit directional system is going to behave in any type of formation. While being very useful, it is likely that this type of modeling is only done in not very known locations due to how time consuming they are.

2.3 Side Cutting

Millheim (1982) undertook a study which was pioneering in relating bit and stabilizer side cutting data to a BHA program to generate displacements in both x and y planes. The input related to the geology consisted of divided layers with an average thickness and a hardness classification (ranging from very soft to very hard). They found that depending on the hardness of the formation, a minimum side force had to be present for the bit to present any side cutting tendencies and that value was also inputted for each layer. The BHA inputs consisted of bit diameter and clearance, as well as collar and stabilizer properties and configurations. In addition, they found that bits have a tendency to cut over overgage holes for all the rocks in the classification hardness, with exception to the very hard rocks. An input related to that also has to be entered (usually a guess of 0.15 inches) and a wrong guess caused instability in the program or

prevented it from creating enough build/drop angle. The inputs necessary related to operating parameters were WOB, RPM and depth increment per side force calculations. Before the simulation could start, the initial wellbore conditions also had to be chosen. After that, the BHA program calculated the side forces and the displacement, through a static, quasi-dynamic (they advise this solution for RPM lesser than 90-120) or full dynamic solution (RPM higher than 90-120 for some kinds of BHA, though avoided due to the high number of iterations required). The ROP can then be calculated or it can be an input data from each depth increment, which was how the authors used. After that, there was enough data to determine the amount of side cutting, which is later corrected for hole size and rock hardness based on data from drilling tests. Further correction was done through a factor multiplier to show downhole conditions. For each depth increment, until the desired interval to be drilled was completed, the bit is moved forward. If the side forces on the stabilizer are higher than the threshold of the formation, the hole is enlarged by an amount for the increment drilled. They found that their simulation gave a good match to inclination values observed on the field, however, when the drilling in the field presented itself with high RPM and bit torque, the direction of the side cutting tendencies of the bit would not match. The simulation also did not show the correct side cutting tendencies when there was a lot of change in the wellbore conditions. They stated that, in the conditions of the model at the time the paper was published, the best use of their simulation was to match field data and then use it for predictive behavior. Their model was crucial in starting to better

understand the relations between BHA, and rock/bit interaction. To this day, the industry is still conducting research on that topic and much of the progress made was due to their initial efforts.

Pastusek, Brackin and Lutes (2005) developed a model for predicting the hole curvature based on the bit and BHA by running tests in a full scale drilling simulator (**Figure 14**) with different parameters and side loads (applied by the hydraulic cylinder connected to the bearing collar).

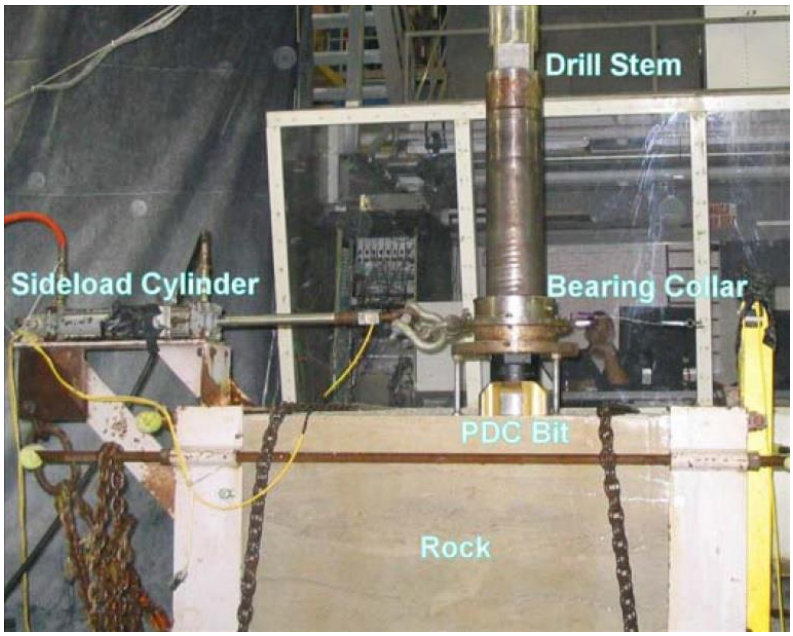

Figure 14 - Schematics of the drilling bench used for the experiments and its respective parts (Pastusek, Brackin and Lutes 2005).

Their tests were conducted in rocks with compressive strength varying from 2,000 psi to 50,000 psi, with the most common being the Carthage limestone

(15,000-18,000 psi). To characterize the bit, they drilled 20 to 40 inches with a constant side load. The side loads varied from 250 to 2000 lbs, and they maintained constant ROP (48 ft/hr) and RPM (120). They had water circulating to simulate drilling fluid and were able to measure depth drilled, WOB, torque and lateral deflection. After the data was processed a plot of depth drilled vs lateral displacement was made. The arctangent of the slope of the resultant line gave the bit tilt (difference between bit and borehole axis – **Figure 15**) in degrees. That result was then plotted vs bit side load, demonstrating the build and the drop (through mirroring the data about the origin) capability of the bit.

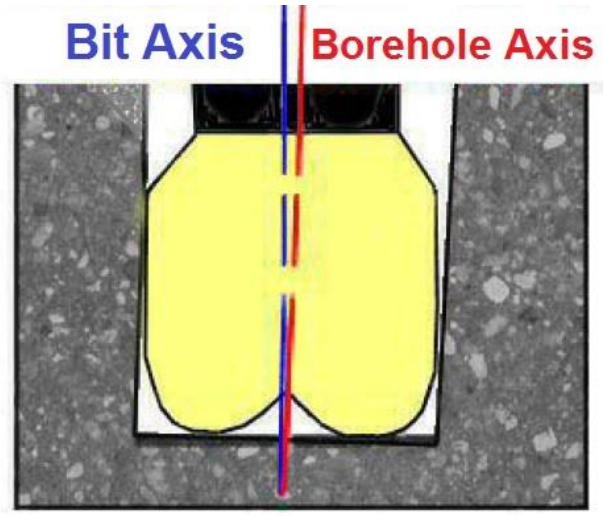

Figure 15 - Bit Tilt schematics (after Pastusek, Brackin and Lutes (2005)).

They used a finite element analysis software to model the BHA based on different BHA configurations as well as wellbore curvatures, which output bit tilt

and side force. The results from the BHA modeling and the bit characterization were then put together on the same plot (**Figure 16**). The intersection between the two trends represents points where the bit aggressiveness and the BHA capabilities are compatible while points on the bit curve that are outside of the BHA response represent conditions where the aggressiveness of the bit surpasses the BHA capability, which can lead to a decreased wellbore quality with no gain in build rate. The model was also verified in field experiments.

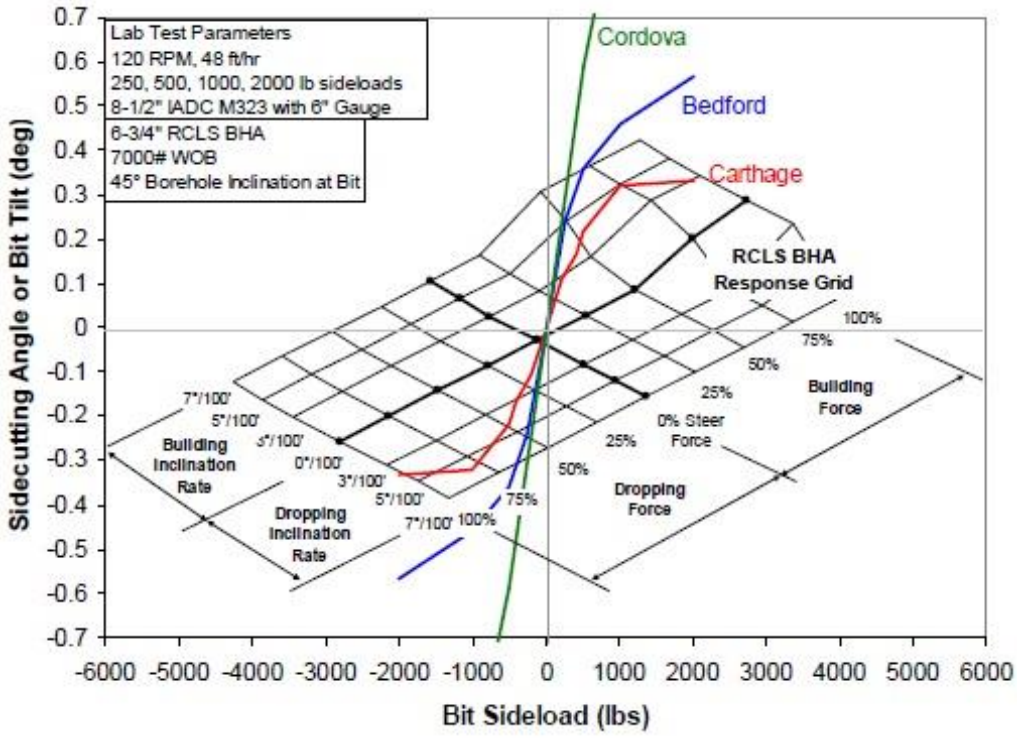

Figure 16 - Results combining finite element analysis and bit response curves (Pastusek, Brackin and Lutes 2005).

Their work was very complete and the only improvement would be to run the tests with varying ROP, RPM and formation anisotropy to account for their influence on the bit steerability. It is very useful in choosing both the bit and the BHA to be used as it compares the aggressiveness of the bit with the capabilities of the BHA, thus preventing the use of very aggressive bit that is going to cause borehole quality problems or allows the use of a more aggressive bit in case the BHA can handle it, which will generate the desired build/drop.

Ernst, Pastusek and Lutes (2007) studied the effects of RPM and ROP on build rate. They used the same full scale drilling bench used by Pastusek, Brackin and Lutes (2005) (***Figure 14***) to simulate the bit tilt and the side loading (provided to the system by a hydraulic cylinder connected to the non-rotating collar) that is normally present during a drilling operation. The set-up also includes a device for lateral displacement. The bit design was the same through all the tests and inspections were conducted to make sure no damage was done to the cutters, which would affect later test results. They recorded the lateral displacement at a high level of accuracy. The controlled environment allowed the tests to take place without inconsistencies usually observed in the field such as vibrations and energy that doesn't reach the bit due to the BHA, formation heterogeneity, borehole quality problems, and unreliable data. The formations used were homogeneous rocks of both medium (6,000 psi of compressive strength) and hard (compressive strength varying from 15,000-18,000 psi) limestone. They used RPM, ROP and sideloads according to **Table 1** and recorded the resultant lateral displacement

and vertical depth drilled. From those values a plot was put together in which the slope of the curve obtained allows calculation of the bit tilt as a function of the side load (as described previously in Pastusek et. al. 2005).

Table 1 - Schematics of the side loads used for each RPM and ROP used in the experiments.

Bedford					Carthage				
		RPM					RPM		
		60	120	240			60	120	240
		500 lbs	500 lbs	500 lbs			500 lbs	500 lbs	500 lbs
	18	1000 lbs	1000 lbs	1000 lbs		18	1000 lbs	1000 lbs	1000 lbs
		2000 lbs	2000 lbs	2000 lbs			2000 lbs	2000 lbs	2000 lbs
		500 lbs	500 lbs	500 lbs				500 lbs	
ROP	36	1000 lbs	1000 lbs	1000 lbs	ROP	36		1000 lbs	
		2000 lbs	2000 lbs	2000 lbs				2000 lbs	
		500 lbs	500 lbs	500 lbs			500 lbs	500 lbs	500 lbs
	72	1000 lbs	1000 lbs	1000 lbs		72	1000 lbs	1000 lbs	1000 lbs
		2000 lbs	2000 lbs	2000 lbs			2000 lbs	2000 lbs	2000 lbs

For the medium strength formation they found that RPM has a substantial influence on the steerability of the bit. An increase in RPM, translates into a significant side cutting angle increase (up to 65% more, depending on the ROP that it was tested on) (**Figure 17**).

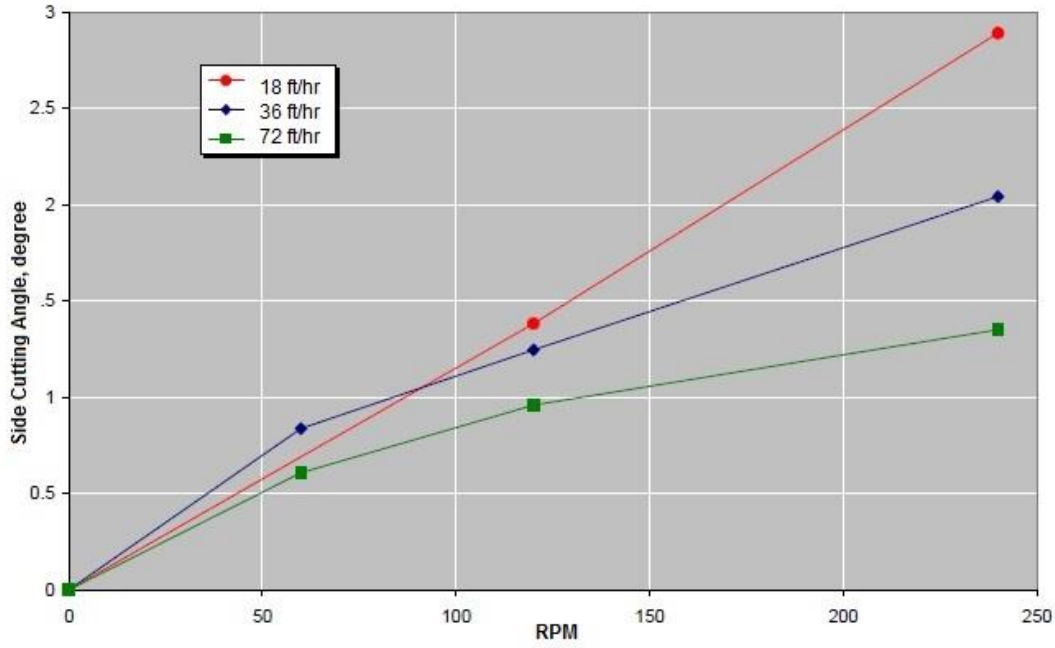

Figure 17 - Side cutting angle vs RPM for the medium strength rock (Ernst, Pastusek and Lutes 2007).

The change in sideload also made a difference in the slope of the side cutting angle vs side load curves, pointing out its influence on bit steerability (**Figure 18**). Those curves showed that the curves from different parameters overlaid each other in some points, which were called points of steerability equivalence, which means that different parameter combinations can provide the same side cutting requirements.

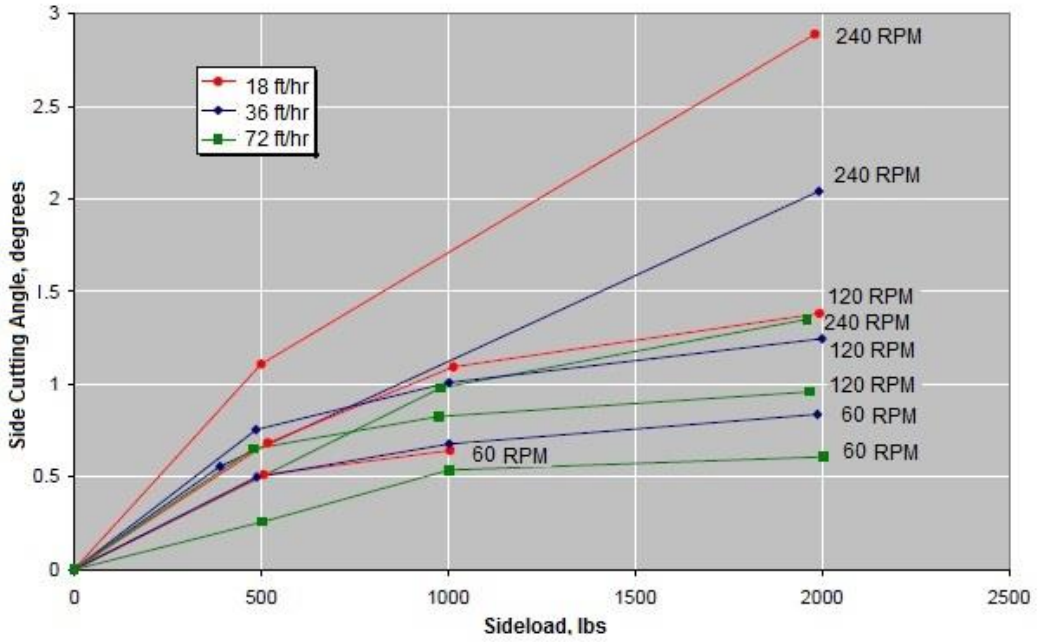

Figure 18 - Side cutting angle vs sideload for the medium strength rock (Ernst, Pastusek and Lutes 2007).

In addition, it was observed that for a constant RPM the cutting angle increased with a decrease of the ROP, and even though those observations are more prominent in higher RPM values, the data shows that ROP has an important role on the bit steerability when associated with RPM (**Figure 19**). The harder rock results presented the same tendency, however, in a lower extent (the increase in RPM got up to an increase of only 35% of steerability, per example). This work is supplement to the work of Pastusek, Brackin and Lutes (2005) and together they provide the biggest influence to the work being developed in this thesis. It would be interesting to see how the bit/BHA would behave in a mixed environment, where there were both soft and hard rocks, and how that anisotropy would influence on the side cutting abilities of the system.

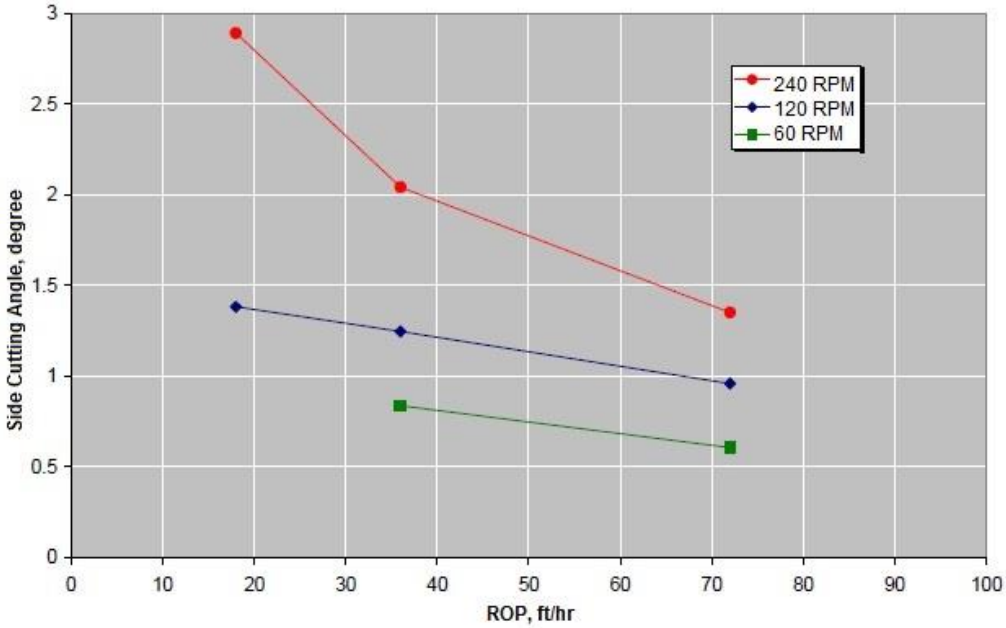

Figure 19 - Side cutting angle vs ROP for the medium strength rock (Ernst, Pastusek and Lutes 2007).

3 METHODOLOGY

This section is dedicated to provide details of the experiments conducted. To do so, the section will be broken down in a discussion on how the samples were made, a description of the rig, detailing its functionalities and the modifications that were necessary to adapt the rig designed by Tingey (2015) to better fulfil the requirements of the present study and a description of the experiments.

3.1 Samples

The concrete samples were made with a compressive strength to simulate the strength seen in real life sandstone formations. The recipe and mix of the concrete were outsourced from Martin Marietta, a company with an office located in Bryan, Texas. The recipe used is describe in **Table 2** below. The compressive strength aimed to achieve was 11,000 psi.

Table 2 - Recipe of the concrete used to do the samples.

Material	Description			Specific Gravity	Weight lbs/yd
Cement	ASTM C150	Type I/II Cement		3.15	750
Alt. Binder	ASTM C618	Class C Fly Ash		2.63	250
Fine Aggregate	ASTM C33	Concrete Sand		2.63	982
Coarse Aggregate	ASTM C33	1" Crushed Stone		2.79	1332
Coarse Aggregate	ASTM C33	#89 Pea Gravel		2.63	529
Water	ASTM C94		32.0 Gallons		267
HR WR	ASTM C494	PS1466			
WR	ASTM C494	PolyHead 997			
				TOTALS	**4109**
	Specified slump	6.50" +/- 1.50"	**Designed unit weight**	152.2 lbs/ft^3	
	Entrapped air	2.0%	**Designed w/cm**	0.27	

The concrete, once ready, was poured on the Flywheel facility of Texas A&M University. In order to fit the shaft of the rig, the samples were designed to have 22" of length and 12" of diameter. 10 samples followed the design previously used by Tingey (2015), with a rebar skeleton to provide more support to the sample. However, considering that the samples used on this study had a considerably higher compressive strength, 11 samples were done without any rebar. Both groups of samples have a row of three polyvinyl chloride (PVC) caps, that act as a screw holding device in order to keep the samples from rotating while being drilled (**Figure 20**). This method was not perfect and failure was noticed in some of the samples (**Figure 21**).

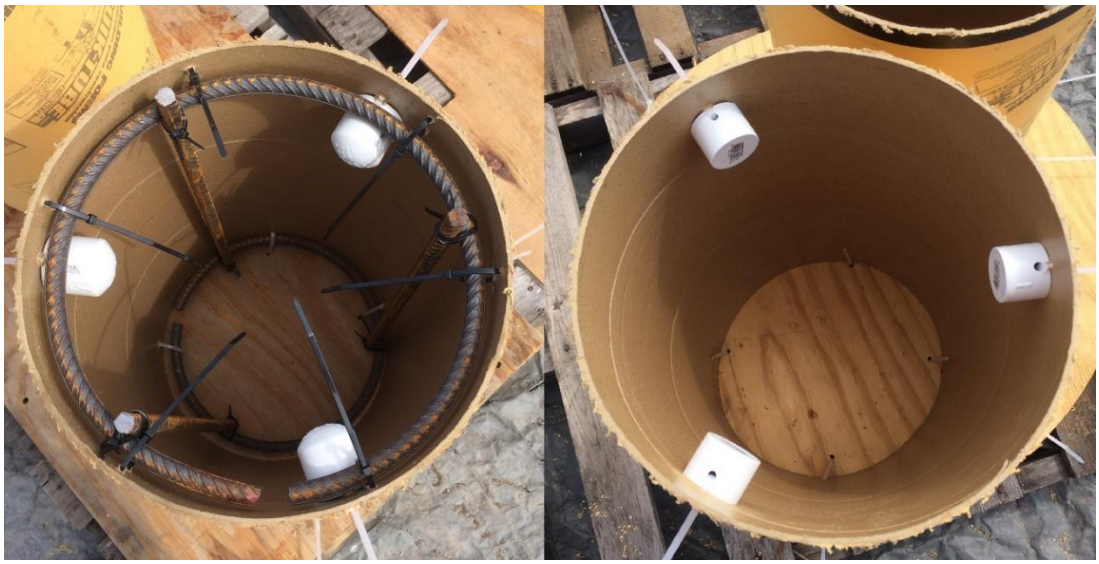

Figure 20 - Design of both groups of samples.

Figure 21 - Failed rotation prevention device

After the concrete had been poured, the samples were watered twice a day and kept covered by plastic for 28 days for the curing period of the cement, and after that they were still watered once every other day for 15 days. During this entire time, the samples were kept covered by plastic in order to keep the humidity of the cement and prevent the samples from cracking. The samples were left in the mold up until being drilled (**Figure 22**).

Figure 22 - Sample after being poured on its mold, where it stayed until being drilled.

In order to verify if the samples achieved the desired strength, they were sent to civil engineering testing firm, Terracon. They tested 3 cores according to the ASTM C-42 standards (one from the top, one form the middle and one from the bottom of the samples), each with 4 in diameter and 12 in of length, and found that the samples had 9180 psi, 8030 psi and 6620 psi of compressive strength from top to bottom. The possible reasons that the desired compressive strength was not achieved is that the watering process used was not effective enough. This theory is corroborated by the fact that the bottom core presented the lower compressive strength, which leads to the conclusion that the water did not reach the bottom of the samples. Another possible reason for the low compressive strengths is the lack of vibration during the pouring of the concrete to liberate the entrapped air.

3.2 Rig

The experimental test rig is located at the Flywheel campus of the Texas A&M University. It consists of a sample carriage, a carriage drive, a shaft drive and a circulating system. Those systems will be briefly described on this section, but more details about the design of the rig are available in the work of Tingey (2015).

The sample carriage (**Figure 23**) is the most complex part of the rig, housing the sample and all the sensors used to measure the loads applied during the tests. The sample is positioned inside a steel cylinder that will be referred to as sample

container that is connected to all load sensors used to provide data for the study, which are a torsional/axial load cell and 8 rods that measure the lateral load applied. The rods are then supported by an outer cylinder that is connected to the frame of the sample carriage. Connected to the outer cylinder is the system that generates the lateral load. It consists of an electric motor connected to a pin that when activated makes contact to the outer cylinder, generating a lateral load to the system. After extensive tests, it was defined that the rods did not provide trustworthy data due to their high sensitivity on temperature. For that reason, all the data collected for this work is provided from the torsional/axial load cell, located at the end of the sample container.

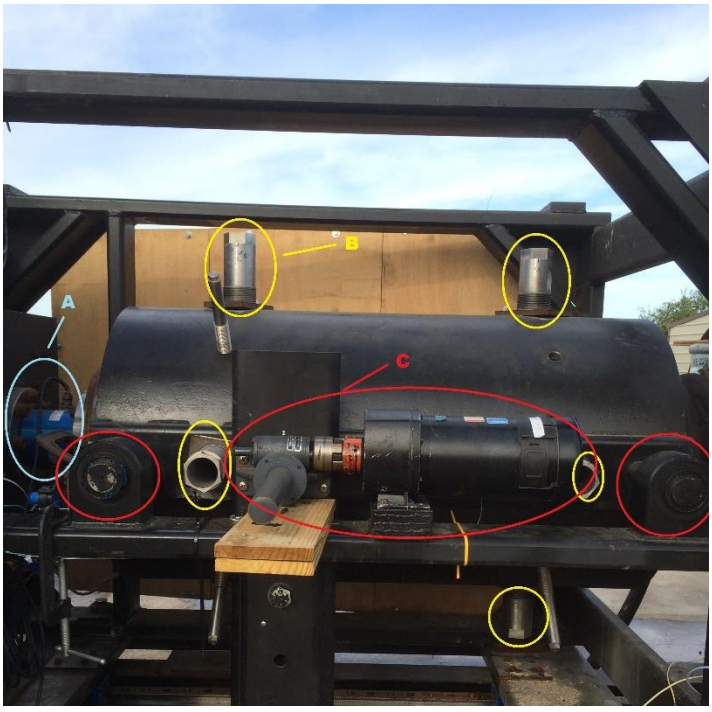

Figure 23 - Picture of the Sample Carriage, detailing the A - Torsional/axial load cell, B - Rods, C - Motor that applies side load.

The carriage drive (**Figure 24**) houses the hydraulic cylinder that provides the WOB necessary for the system to push the formation sample into the bit. The WOB can be roughly controlled by a valve that dictates the amount of fluid that is going to be liberated to the hydraulic system. This system is powered by a deep cycle marine battery.

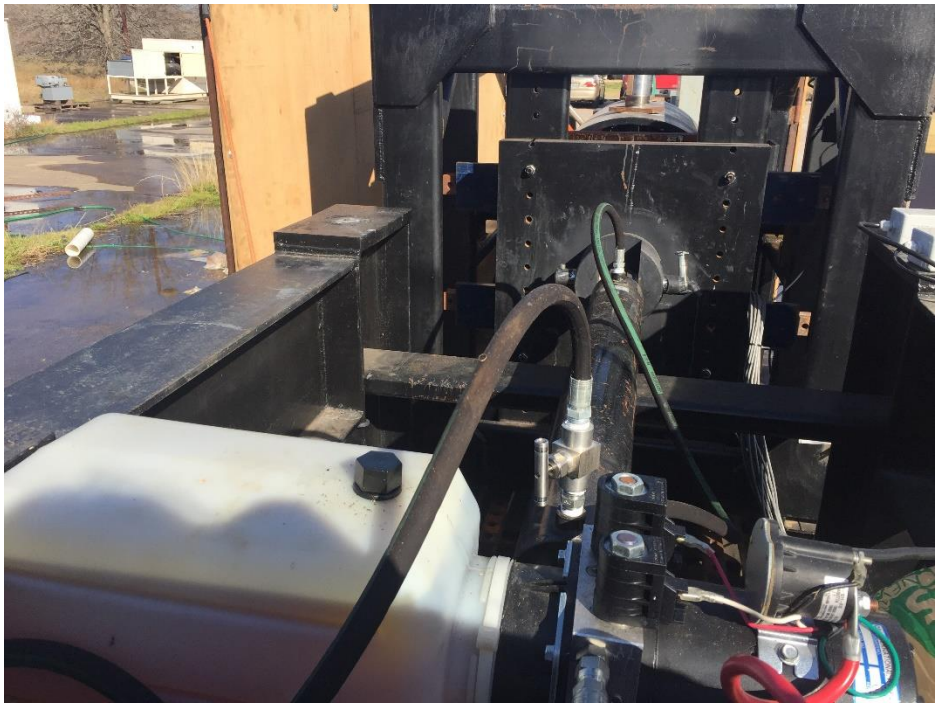

Figure 24 - Carriage drive system of the rig.

The shaft drive (**Figure 25**) consists of the drive motor, a speed reducing gear box, the drill shaft, a crossover and the drill bit, and the main purpose of the system is to provide the necessary RPM for the bit to drill the sample. The bit (**Figure 26**) used was a 6” diameter PDC bit from Ulterra.

Figure 25 - Shaft drive system of the rig.

Figure 26 - Detail of the crossover and bit.

The circulating system (**Figure 27**) consists of a mud tank, a centrifugal pump, a mud drain and a sediment filter. The fluid used to simulate the drilling fluid was water due to the easy access and disposable procedure. The mud drain is what prevents the fluid from coming out of the sample container and it is connected to the sediment filter through a hose.

Figure 27 - Circulating system of the rig.

The sediment filter (**Figure 28**) consists of a 200 gallon tank that receives the pressurized water from the sample container. The flow is interrupted by simple concrete bricks that act as a kinetic barrier, slowing the cuttings from the sample down. The pipe that connects the sediment filter to the mud tank is covered by a mesh filter to keep the cuttings from going to the mud tank and, consequently,

back into the drilling system. This system had to be adapted from the one used in Tingey (2015) due to the significantly higher compressive strength of the samples used on this project. The previous system clogged and overflew, due to the amount of cuttings generated by a longer drilling period that the higher strength rock required, which was resolved by putting a bigger sediment filter in place.

Figure 28 - Sediment filter in detail.

3.3 Experiments

The experiments were run according to the matrix shown in **Table 3**.

Table 3 - Matrix describing the desired values for WOB, RPM and side loads used during the experiments.

RPM / WOB	60	90	120	
3600 lbs	500 lbs	500 lbs	500 lbs	**Side Loads**
3600 lbs	1000 lbs	1000 lbs	1000 lbs	
3600 lbs	1500 lbs	1500 lbs	1500 lbs	
4700 lbs	500 lbs	-	-	
4700 lbs	1000 lbs	-	-	

The software used to record the data was National Instruments' LabVIEW. The code was the same used in Tingey (2015), with a few adjustments. Because the rods did not provide reliable data, a new way to find side load was necessary. That was done with the help of the Biomedical Engineering Department at Texas A&M University, where their program for tracking artery dilation was adapted to find the deflection of the shaft when a force was applied to it. The program works with a correlation from pixels from the image of an HD Webcam and the distance that the shaft moved.

The shaft deflection was calibrated as illustrated by **Figure 29**. Forces measured by a scale were applied to the shaft and the deflection shown by a dial indicator positioned exactly where the camera should be located. The forces and deflections recorded are shown in **Table 4** which were plotted (**Figure 30**). A linear adjustment was made in order to find an equation that was used on the Labview

program. As mentioned before, the program correlates the amount of pixels with deflection and the linear equation was used to predict the lateral force being applied to the shaft, so that it could be controlled in real time.

Figure 29 - Schematics of the calibration done to find the force equation for the LabVIEW program.

Table 4 - Forces and Deflections read during the calibration of the shaft.

Force (lbs)	Deflection (in)
27	0
95.5	0.005
168.5	0.01
225	0.015

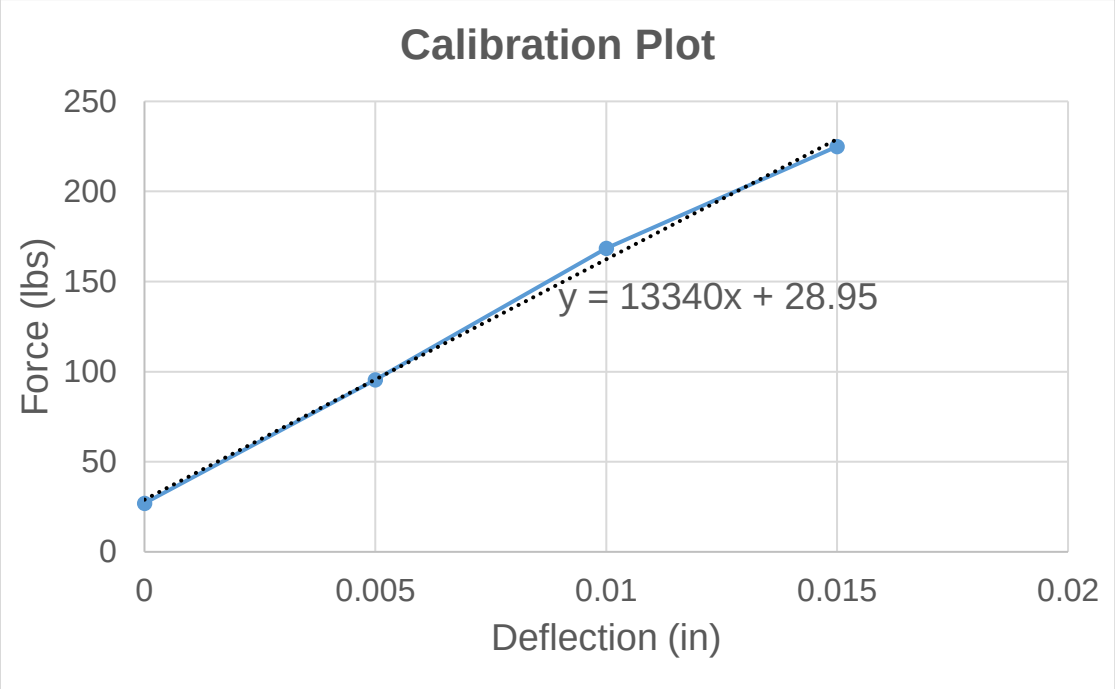

Figure 30 - Plot generated with the data from the calibration of the shaft (Deflection X Force).

3.4 Data Processing

After the experiments were done, the data was retrieved from the .txt file generated by the LabView program and put into a Microsoft Excel spreadsheet, where the data was refined and processed.

The data that was recorded before the bit made contact to the sample (due to a delay between the time the data began being recorded and the time the drilling started) was deleted and the time stamp was adjusted by using the recording interval of the data. The depth drilled was also adjusted, using the first recorded value as a zero and subtracting that from all the other recordings. The same had to be done for the lateral displacement, as both measurements were done by the same type of sensor (a string potentiometer).

The ROP and the MSE were *calculated* by the following equations:

$$ROP = \frac{Depth\ Drilled}{Time\ Drilled} \quad (1)$$

$$MSE = \frac{480 * TOB * RPM}{ROP * D^2} + \frac{4 * WOB}{\pi * D^2} \quad (2)$$

Where,

ROP = rate of penetration

MSE = mechanical specific energy

TOB = torque on bit

RPM = rotation per minute

WOB = weight on bit

D = bit diameter

When there is a side load applied to the shaft, it will cause the shaft to bend and to point the bit to a different direction. So in order to find the deflection caused by the sidecutting abilities of the bit, those facts have to be taken into account as seen in **Figure 31**.

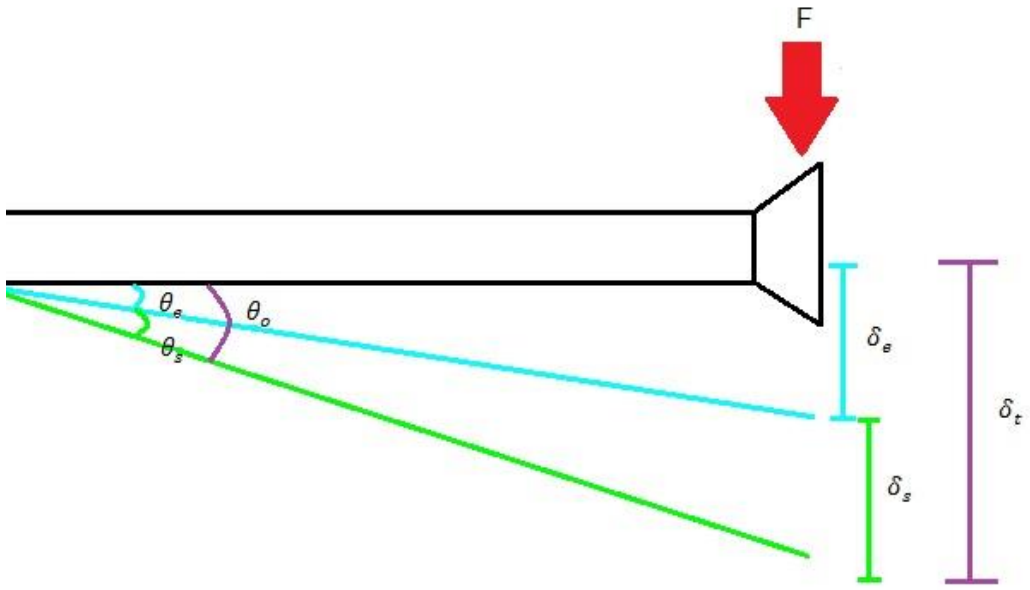

Figure 31 - Break down of the deflections and angles accounted for when there is a side load applied to the shaft where δ_e is the deflection predicted by the Euler equation, δ_s is the deflection caused by side cutting, δ_t is the total deflection, θ_e is the angle predicted by the Euler equation, θ_s is the angle caused by side cutting and θ_o is the overall angle.

To account for the deflection of the shaft the Euler equation for a fixed cantilever beam was used:

$$\delta_e = \frac{F}{6*E*I} * (l^3 - 3 * L^2 * l + 2 * L^3) \quad (3)$$

Where:

δ_e = deflection as predicted by Euler's equation

F = force

E = Young's Modulus of shaft

I = Moment of Inertia

l = Distance from the shaft origin

L = Total length of the shaft

The Young's Modulus for AISI 4340 steel (material that the shaft is made of) is of $30 * 10^6$ psi and the length of the shaft is 73.25 in. The moment of intertia can be calculated through:

$$I = \frac{\pi}{4} * (R^4 - r^4) \quad (4)$$

Where:

r = internal radius of the shaft

R = external radius of the shaft

However, the Euler equation was not matching up with the calibration points obtained by the experiment on **Figure 29**. A closer look at the experiment and the equation assumptions lead to a couple of hypothesis as to why the responses where not the same:

1. The shaft is not homogeneous, having different diameters (**Figure 32**) and being composed of different materials (shaft itself, crossover and bit);

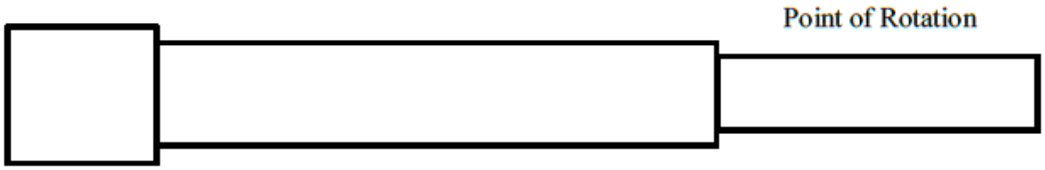

Figure 32 - Model of the drill shaft (after Wilson (2013)).

2. The bearings attaching the shaft have some play to it, making the shaft not behave exactly like a fixed cantilever beam, as shown by the **Figure 33**.

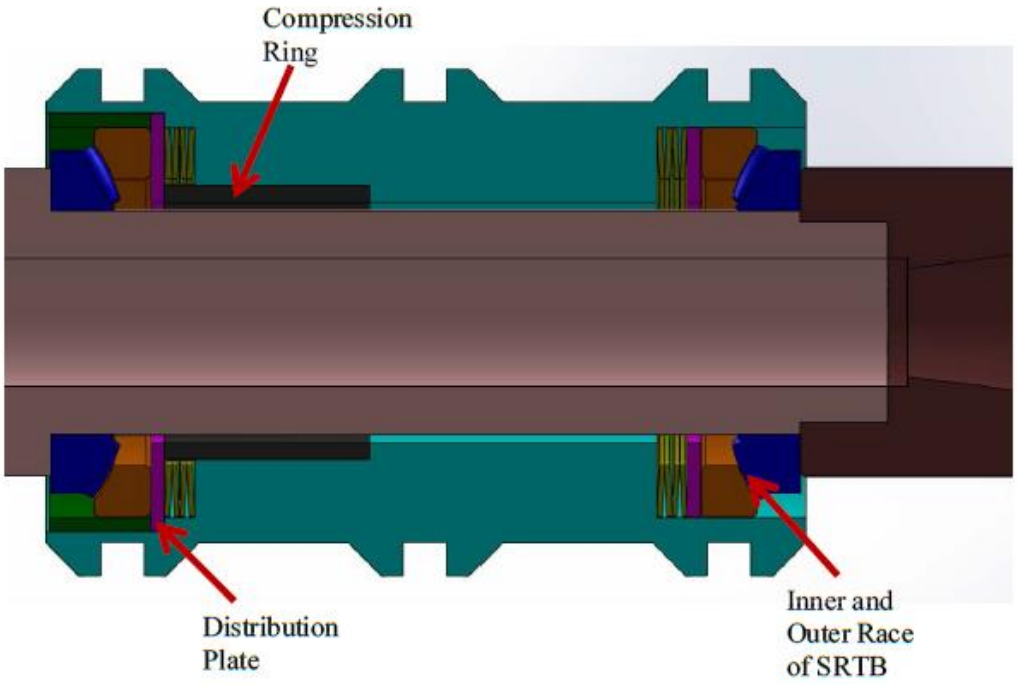

Figure 33 - Schematics showing the shaft support configuration (after Wilson (2013)).

To account for the second hypothesis, the difference in the deflection between the theory and the calibration was found and plotted versus the forces used for the calibration, which resulted in a linear trend. Considering that the forces used for calibration were a lot smaller than the forces used during the experiments and that the deflection of the shaft tends to become more asymptotic, a logarithmic trendline forecasting a side load of 3000 lbs was created (**Figure 34**).

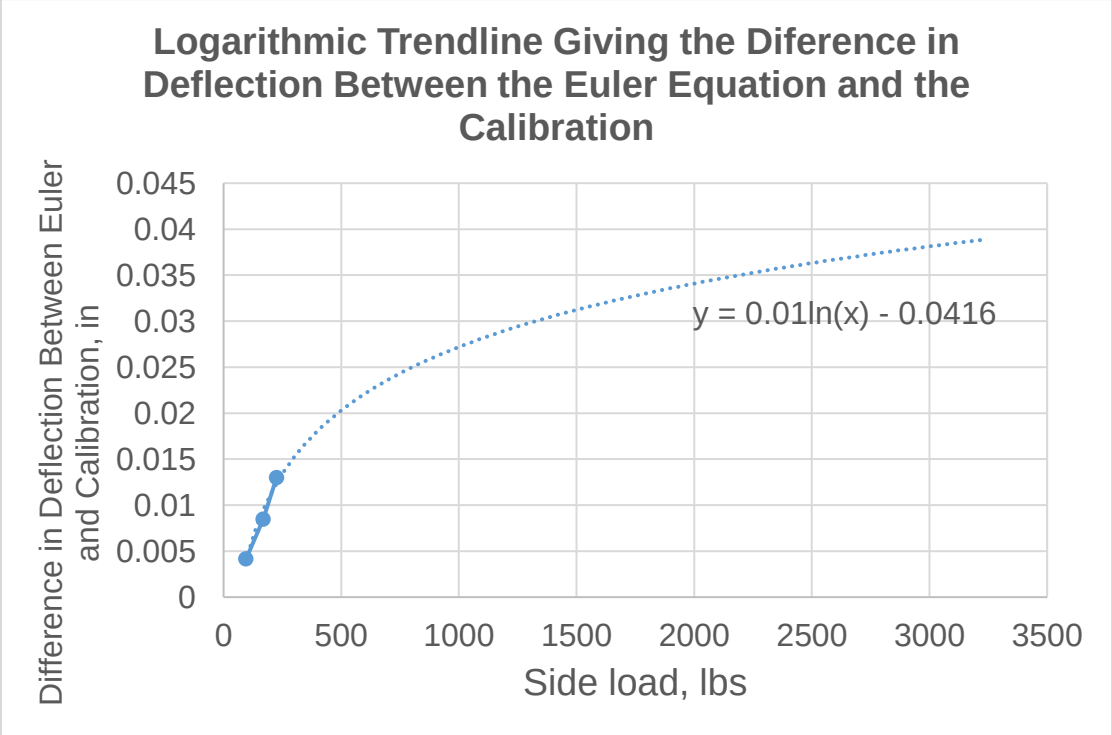

Figure 34 - Plot of the difference in deflection between the Euler equation and the calibration versus side load, resulting in a logarithmic trendline to be applied as a correction for the Euler equation.

The equation for the trendline was then added to the Euler equation, providing a correction that matched the theory to the calibration (**Figure 35**).

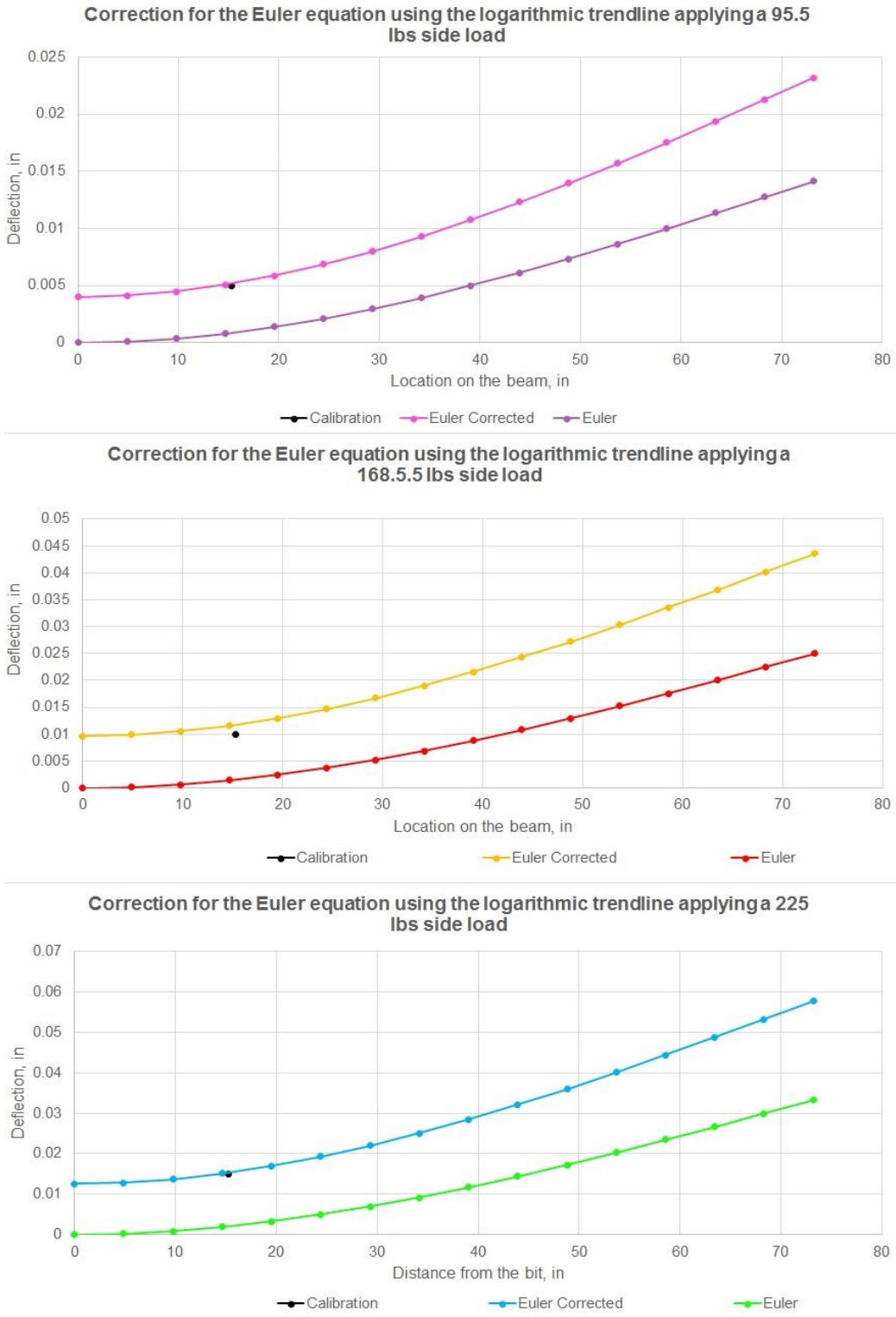

Figure 35 - Graphs showing the correction of the Euler equation, applying the logarithmic trend, accounting for the bearing play and better matching the calibration, for each force during the calibration.

The modified Euler equation that provided the fit above and that was used throughout this thesis was the following:

$$\delta_e = \frac{F}{6*E*I} * (l^3 - 3 * L^2 * l + 2 * L^3) + 0.01 * \ln(F) - 0.0416 \quad (5)$$

With that equation it was finally possible to calculate the deflection due exclusively to the sidecutting abilities of the bit.

$$\delta_{sc} = \delta_{mc} - \delta_{ec} \quad (6)$$

$$\delta_{sb} = \delta_{mb} - \delta_{eb} \quad (7)$$

Where,

δ_{sc} = deflection due to sidecutting at the camera

δ_{mc} = deflection measured at the camera

δ_{ec} = deflection predicted by Euler's equation at the camera

δ_{sb} = deflection due to sidecutting at the bit

δ_{mb} = deflection measured at the bit

δ_{eb} = deflection predicted by Euler's equation at the bit

It is important to note that Equations 3 and 6 present a different sign convention than the one presented by Hibbeler (2013) (**Figure 36**). For that reason, all data referring to side load had to be mirrored (**Figure 37**), in order to follow the convention, which is the way this parameter will be presented.

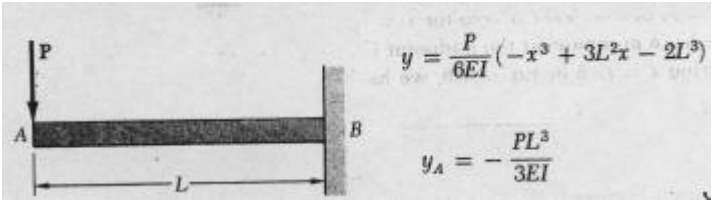

Figure 36 - Convention of signs followed on the present study for deflection and side load ((Hibbeler 2013)).

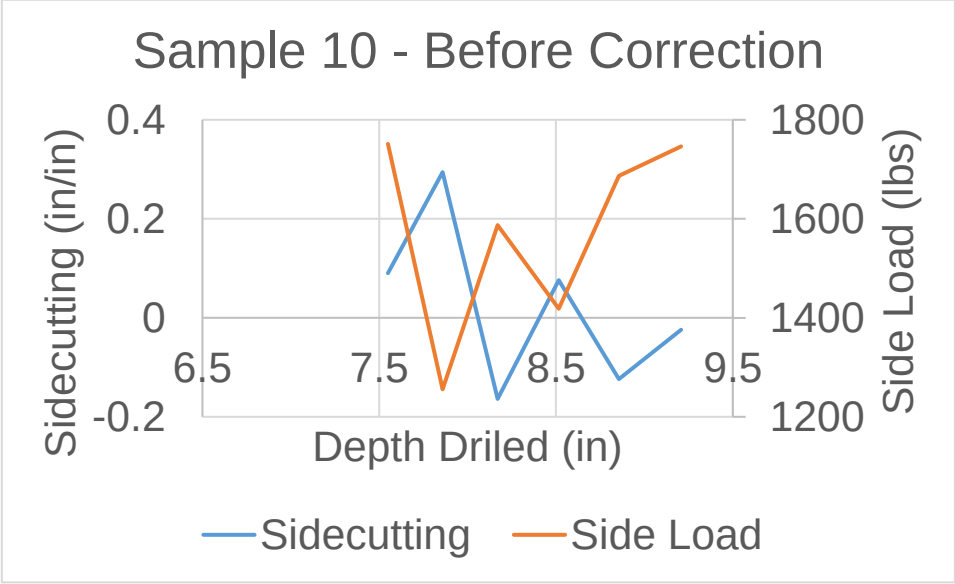

Figure 37 - Example of a plot of sidecutting and side load before the correction of sign convention was applied.

The side cutting angle was calculated following the procedure done by Pastusek, Brackin and Lutes (2005), where a plot of depth drilled versus lateral displacement was done and a linear fit was found. The arctangent of the slope of the curve was then found in order to find the desired angle. An example of the result of the procedure is illustrated by **Figure 38**. However, considering that the WOB and side load were not constant during the experiments of the present work,

as they were on the paper mentioned, the data used for calculation of the side cutting angle had to be chosen from part of the sample. The pool of data used for each sample differed and had to be chosen at the parts of the drilling operation where both WOB and side load were maintained relatively constant for longer.

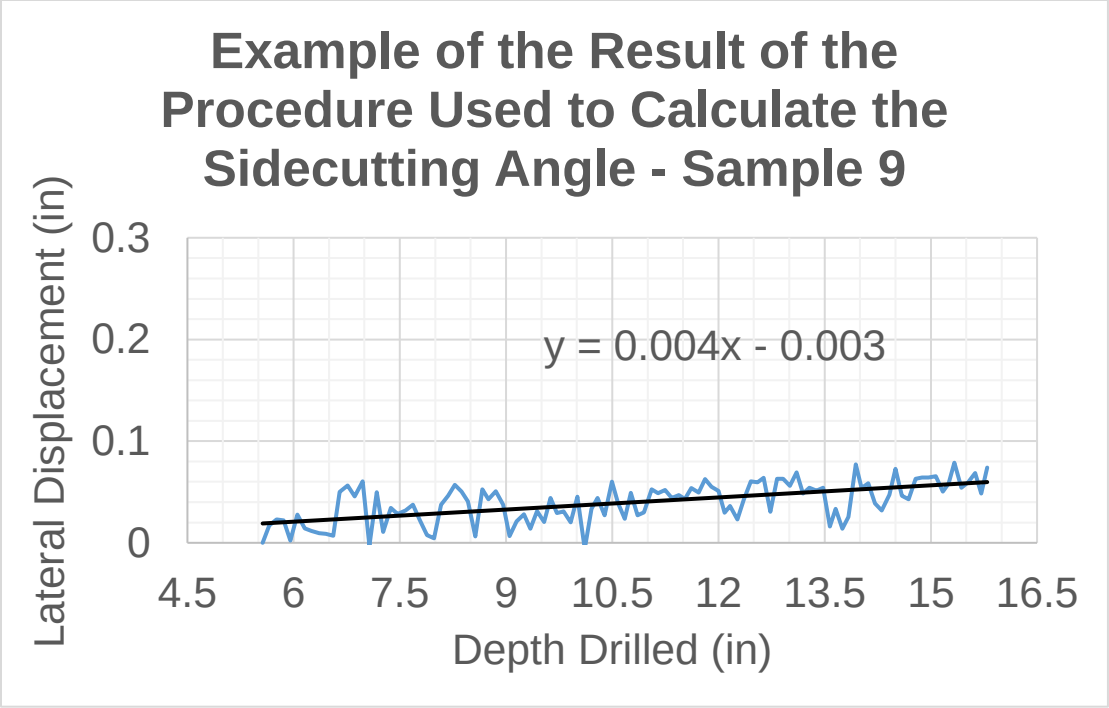

Figure 38 - Example of the result of the procedure done to all samples to find the side cutting angle from the slope of the trendline generated by the plot of the lateral displacement versus depth drilled.

4 RESULTS AND DISCUSSION

4.1 Results

From the twenty-one samples made, one was used for testing (as explained in Section 3.1), one was deemed unfit for use due to the poor finishing, leaving the part around of the rebar lacking concrete (**Figure 39**) and six were used to refine the rig capabilities. As mentioned before (on Sections 3.2 and 3.3), quite a few changes were made to the rig. The circulation system needed a bigger sediment filter, the rod sensor system for acquiring information proved to be untrustworthy requiring the measurements of WOB and TOB to be done through the load cell. However the side load measurements were still unsatisfactory, so the HD webcam was installed, providing a more accurate side load and giving a shaft deflection, which was used to correct the deflection due to sidecutting. Through this extensive process of adapting the rig nine samples were drilled and could not be used as data sets.

Figure 39 - Picture of the sample with poor finishing, where the detail shows the lack of concrete around the rebar

Other problems faced during the drilling operations were in controlling the side load and the WOB. The rig did not have an automated system to regulate those parameters, so everything had to be done manually. This posed a challenge and the parameters were not as constant as one would like. The best way to try and control them was having one person designated to be at the hydraulic valve that controlled the WOB and one person designated to control the motor that applied side load at all times. They were provided with a computer screen and were able to observe on real time the changes on the parameters, thus being able to respond accordingly with the least delay in time.

This left Samples 1 through 13 to capture results (**Table 5**), however, there was more problems during drilling. On Sample 1, the string potentiometer responsible to acquire the depth of drilling stopped giving measurements. We

noticed that one of the cables connecting the sensor to the DAQ came loose and were able to fix it with no problem for the following samples.

Table 5 - Description of the samples used for testing and their respective desired drilling parameters and side cutting results

Sample	Test Date	WOB (lbs)	Side Load (lbs)	RPM	Comments
1	07/19	2500	500	60	Motor overheated and string sensor got disconnected
2	07/25	3600	500	60	Problem with string sensor
3	07/25	3600	500	90	Problem with string sensor
4	07/26	3600	500	120	Problem with string sensor
5	07/26	3600	1000	60	Problem with string sensor
6	07/26	3600	1000	90	Problem with string sensor
7	07/26	3600	1000	120	Problem with string sensor
8	8/3	3600	1500	60	Problem with string sensor
9	8/5	3600	1500	60	Cleared for analysis
10	8/5	3600	1500	90	Cleared for analysis
11	8/8	3600	1500	120	Cleared for analysis
12	8/8	4700	500	60	Cleared for analysis
13	8/8	4700	1000	60	Cleared for analysis

Another problem observed during drilling was the pump and motor that power the hydraulic system which applies WOB were overheating. Our diagnosis was that the pump and the motor could not sustain the amount of work for the time we needed. In order to achieve the original desired WOB of 2500 lbs, the

valve that controls the fluid from the hydraulic system was barely opened and the amount of work required for the pump to pass fluid for such a restrained space and during the time needed to drill through the sample caused the system to overheat. Once the WOB was increased, the valve was not as restrained, making it easier for the fluid to flow. As the rig was designed for a much lower sample compressive strength, the time required for drilling through those were a lot lower. To fix that problem we increased the WOB, which increased the ROP and decreased the amount of time spent drilling. We went from a WOB of 2500 lbs to 3600 lbs. Increasing the ROP allowed for the pump and motor to work for a lesser amount of time by opening the valve that allows for the hydraulic fluid to travel, also making the process less demanding.

Drilling operations for Samples 2 through 7 were completed without any of the previous problems occurring. However the string potentiometer which recorded the lateral displacement on the sample output inconsistent readings. Upon inspection the sensor was found to be defective, and was reading zero or near zero values. The conclusion was that the sensor malfunctioned and for some reason did not record. Due to the graphical interface setup for control and sensor readout, the error went unnoticed. As the string sensor measurements are critical in providing input for calculating the side cutting, analysis was not able to be completed for these samples. This sensor was replaced and after that no more problems were seen for this particular measurement.

Sample 8 had a problem with the connection of the string potentiometer to the DAQ, preventing the recording of the part of the data set that accounted for the depth in drilling. This prevented an accurate analysis due to lack of relation of the data that was recorded to the location of it in the sample. This particular problem had presented itself before, on Sample 1, and the reason for it to continue happening was due to the set up of the rig. In order to have enough room to change the samples, the string potentiometer must be disassembled from its housing. Considering how fragile the connections are, it is not surprising that the wires broke. After this happened for the second time, a lot more care was taken and the readings were tripled checked to see if they were actually being recorded.

The remaining samples, 9 through 13, each had full datasets available for data analysis. However, as it has been noted, there were some difficulties in maintaining a constant WOB and side load. For that reason, **Table 6** was created, showing not only an average of the parameters, but also a range of the values obtained for each parameter when WOB and side load were considered to be under control.

Table 6 - Average and range of parameters obtained for each sample during the drilling operations

RPM			WOB (lbs)	Side Load (lbs)	ROP (ft/hr)	MSE (psi)	θ_s (degrees)
Sample 9	60	**Minimum**	3244	1046	30	47310	0.2292
		Maximum	3979	1592	34	69788	
		Average	3698	1346	32	59682	
Sample 10	90	**Minimum**	3187	1249	46	56529	0.8651
		Maximum	3909	1755	47	66142	
		Average	3568	1473	46	60759	
Sample 11	120	**Minimum**	3196	1653	90	28918	1.117
		Maximum	4198	2477	106	43807	
		Average	3680	1963	99	36061	
Sample 12	60	**Minimum**	4693	246	47	49650	0.06303
		Maximum	5077	677	47	59084	
		Average	4899	404	47	52964	
Sample 13	60	**Minimum**	4195	760	45	41639	0.1891
		Maximum	4750	1168	47	55751	
		Average	4497	975	46	48583	

Figure 40, **Figure 41** and **Figure 42** represent a graphical view of WOB, side load and MSE, once WOB and side load considered to be under control. Those were the intervals used for analysis in the present paper. It is important to note that even when the values were considered under control and constant enough

for analysis, there was still a wide range of values. Also, plotting only the constant intervals allow for an idea of what depth drilled was analyzied for each sample.

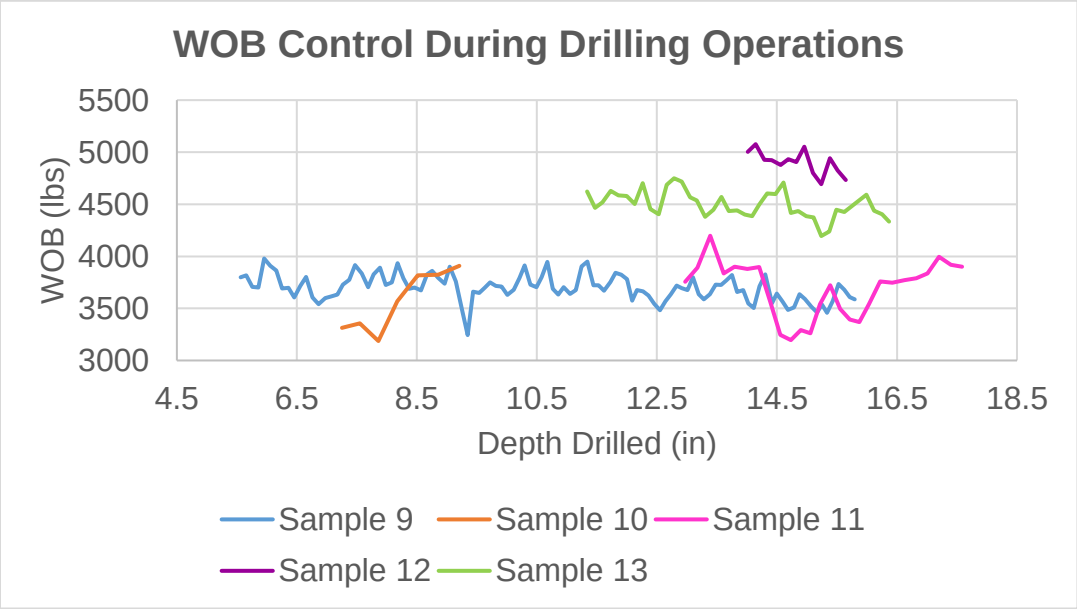

Figure 40 - Graphical representation of the control of the WOB. The depths plotted are equivalent to where the values of WOB and side load were considered constant and were the intervals used for analysis.

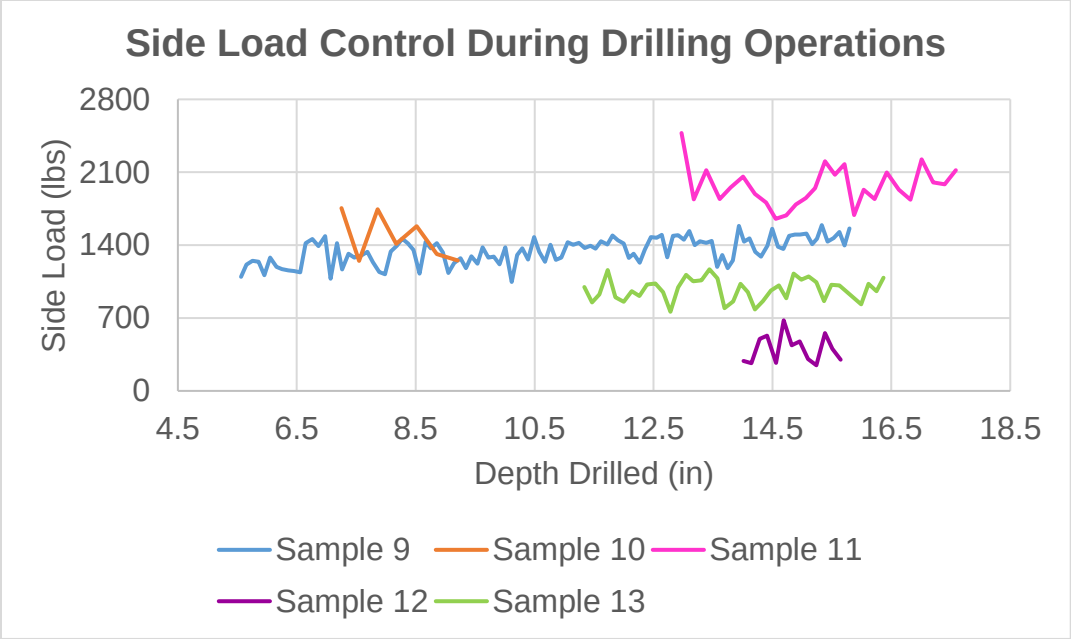

Figure 41 - Graphical representation of the control of the side load. The depths plotted are equivalent to where the values of WOB and side load were considered constant and were the intervals used for analysis.

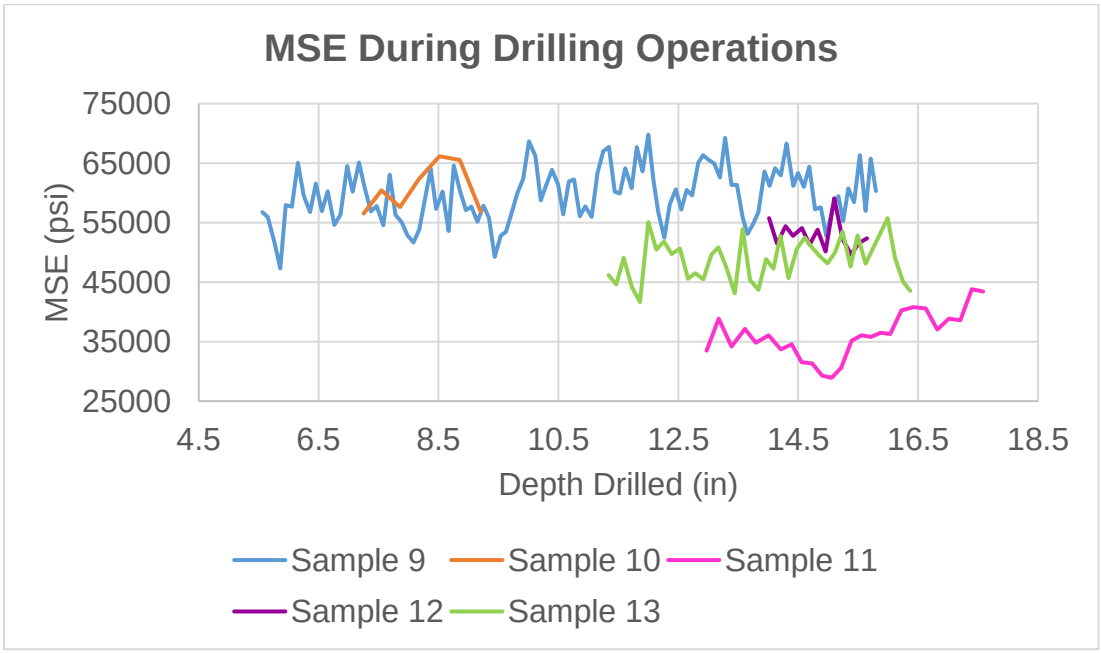

Figure 42 - Graphical representation of the MSE during the operation. The depths plotted are equivalent to where the values of WOB and side load were considered constant and were the intervals used for analysis.

Figure 43 shows the amount of footage drilled at a constant WOB and side load. It is possible to observe that Samples 9, 12 and 13 had the lowest variation on WOB, while Sample 11 presented the highest variation. Sample 12, however, had the lowest side load and those values proved the hardest to maintain constant, thus the short footage drilled for that particular sample. Sample 10 also presented a low footage drilled, due to the fact that side load decreased beyond the desired value and it was not possible to regain it in the short amount of time it took for the sample to be drilled. Therefore it is possible to observe that the parameters became increasingly harder to control with the increase on RPM, likely due to the higher presence of vibration which could have interfered with the sensors.

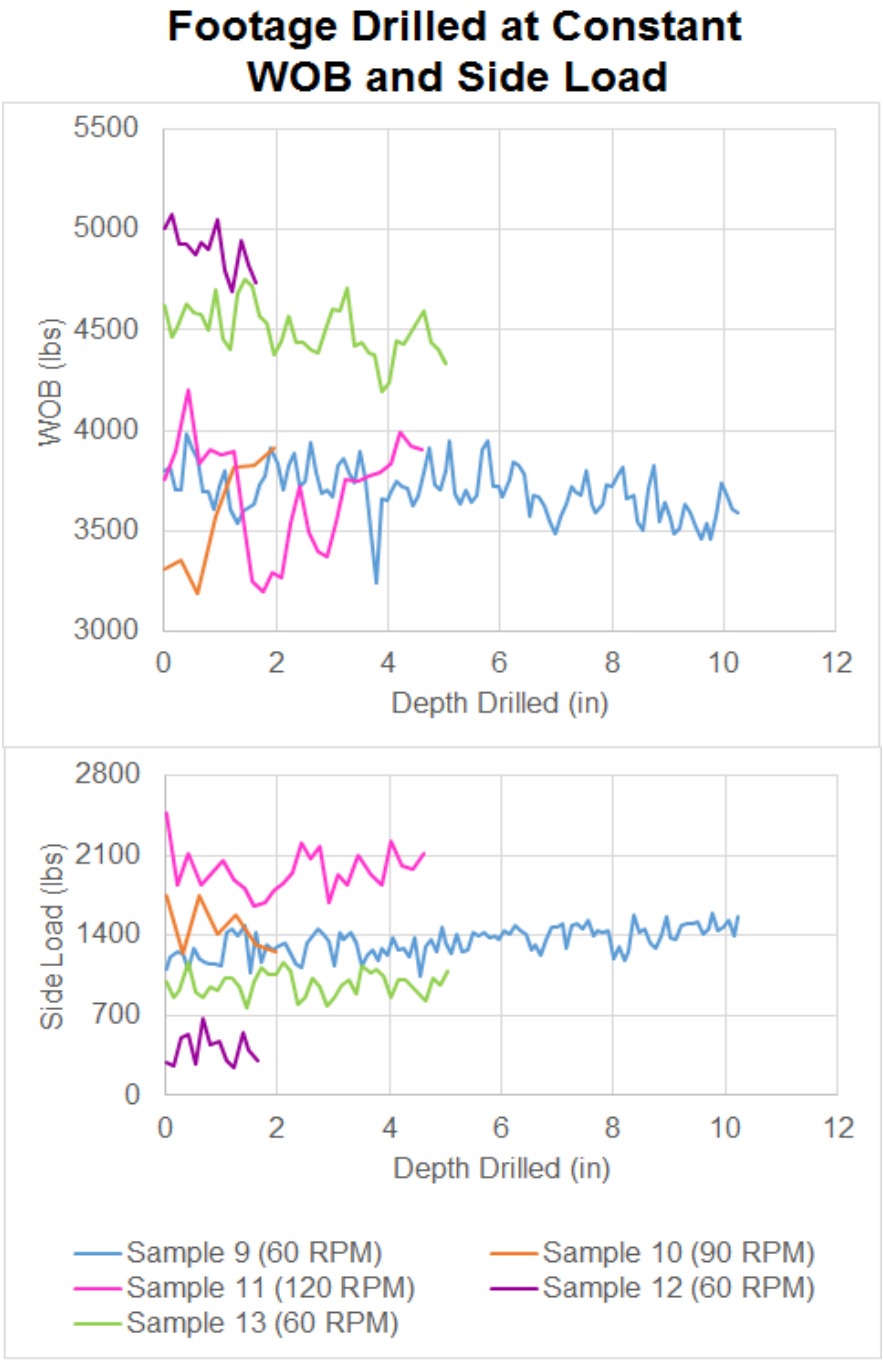

Figure 43 - Increasing noise and wider ranges of applied drilling parameters illustrate the increasing difficulty of system control with increasing RPM. Parameters are plotted over depth of each sample where sideload was considered the most consistent.

Those results were used to investigate the influences generated by side load, RPM, WOB, ROP, and MSE. A discussion and a comparison to the work done in Pastusek, Brackin and Lutes (2005) and Ernst, Pastusek and Lutes (2007) will be presented in the following pages.

4.2 Discussion

Out of all the five samples cleared for analysis, Sample 9 was the one where the control of side load and WOB were achieved for the longest length, providing the largest amount of useful data. For that reason, Sample 9 was chosen as the reference sample and all the other samples were compared to it. The trends for lateral deflection measured for each sample is displayed in **Figure 44**. The R^2 values are low due to the variation in the data. As mentioned before, the control of WOB and side load were a challenging part of the present work and the variation in side load directly affected the lateral deflection. That variation made it harder to fit the data into the desired trendline to calculate the sidecutting angle for each sample. With more samples a method could have been developed to account for varying sideload in the sidecutting angle. However, with the limited number of samples available, attempting to develop a more advanced analysis technique would have led to as much, if not more error and uncertainty.

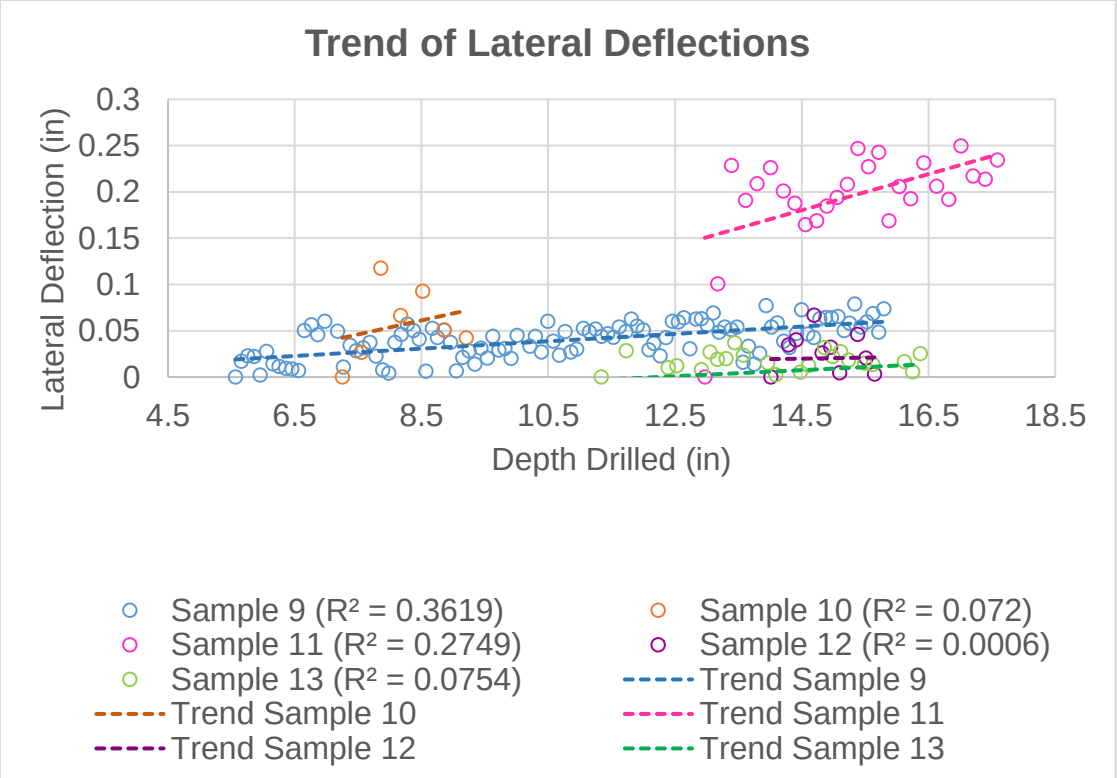

Figure 44 – Graph showing the trend of the lateral deflection for each sample, where it is possible to see the slight increase of lateral deflection as the samples are drilled.

As mentioned in Section 3.4, the side cutting angle for each sample was calculated by finding the arctangent of the slope of the linear trend in the plot between lateral deflection and depth drilled. The plots for all samples are in detail in (**Figure 45**).

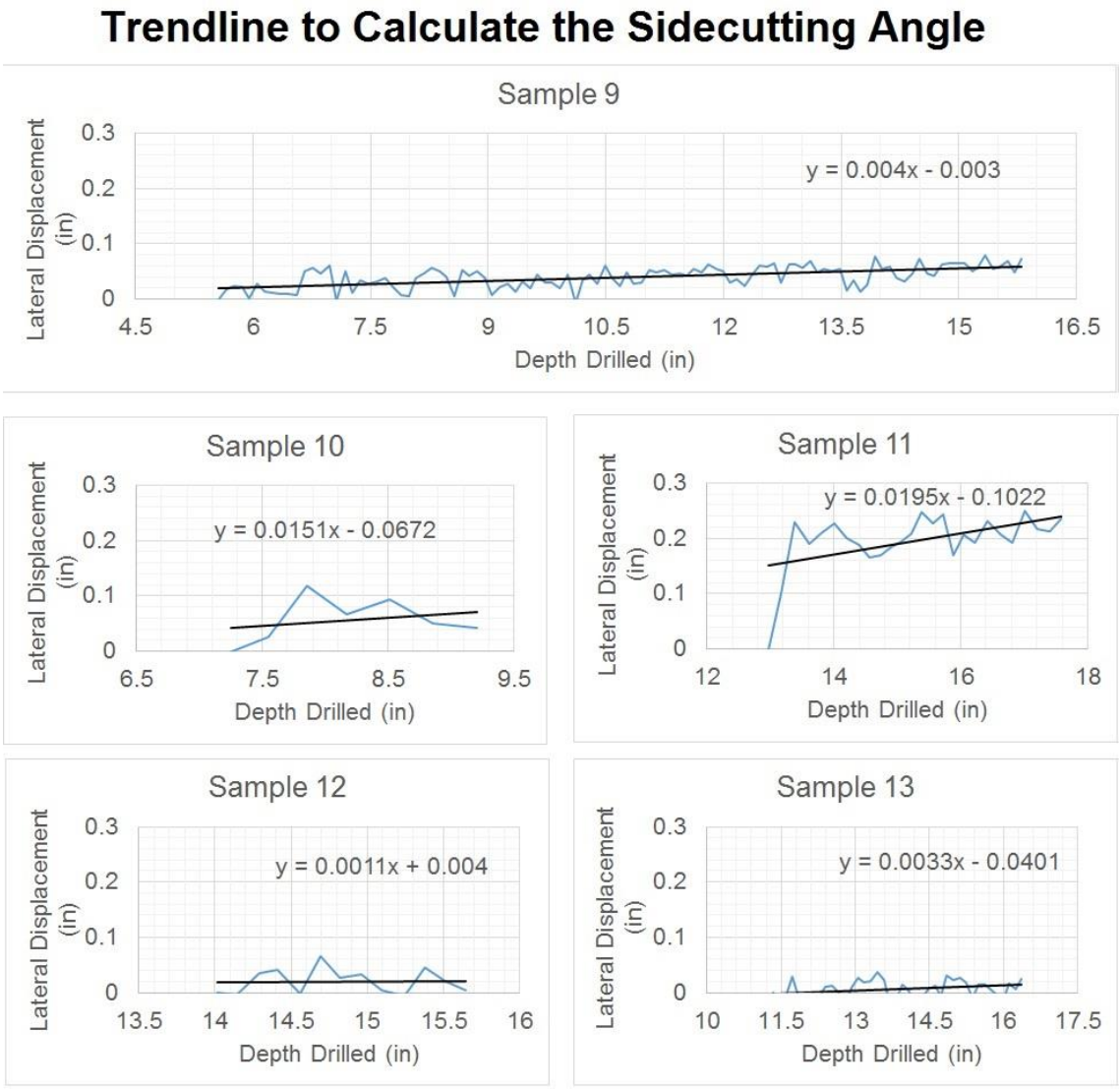

Figure 45 - Slopes of trend lines show the order of samples from smallest to highest angles, or sidecutting to be: 12 < 13 < 9 < 10 < 11.

Analyzing the changes in side loads, it is possible to see that sidecutting and side load follow a very similar trend, for all the samples. Their relationship is very intuitive, as the more force you apply to a body, the more said body will deflect. Considering Samples 9, 12 and 13, where the RPM was maintained at 60

RPM, it is possible to evaluate the side load difference presented in those samples. Sample 12 had a decrease of 70% on the side load from Sample 9, the biggest decrease amongst the samples, resulting on the smallest sidecutting angle, resulting in a decrease of 72.5% in sidecutting when compared to Sample 9. Sample 13 had a decrease of 27.5% on the side load, which resulted in a decrease of 17.5% on the sidecutting angle. In a micro scale within the sample, it is possible to observe that the trend in sidecutting follows the trend in side load, which is illustrated on **Figure 47** and it is corroborated by the relationships found on the work of Ernst, Pastusek and Lutes (2007). **Figure 48** shows results from their work on how the side cutting angle increases for a constant RPM and ROP according to the side load. It is worth to note that both graphs show the sidecutting angle increasing at a higher rate for lower side loads, and becoming asymptotic as the force increases for a constant RPM, showing that the sidecutting angle and side load relate in a logarithmic fashion.

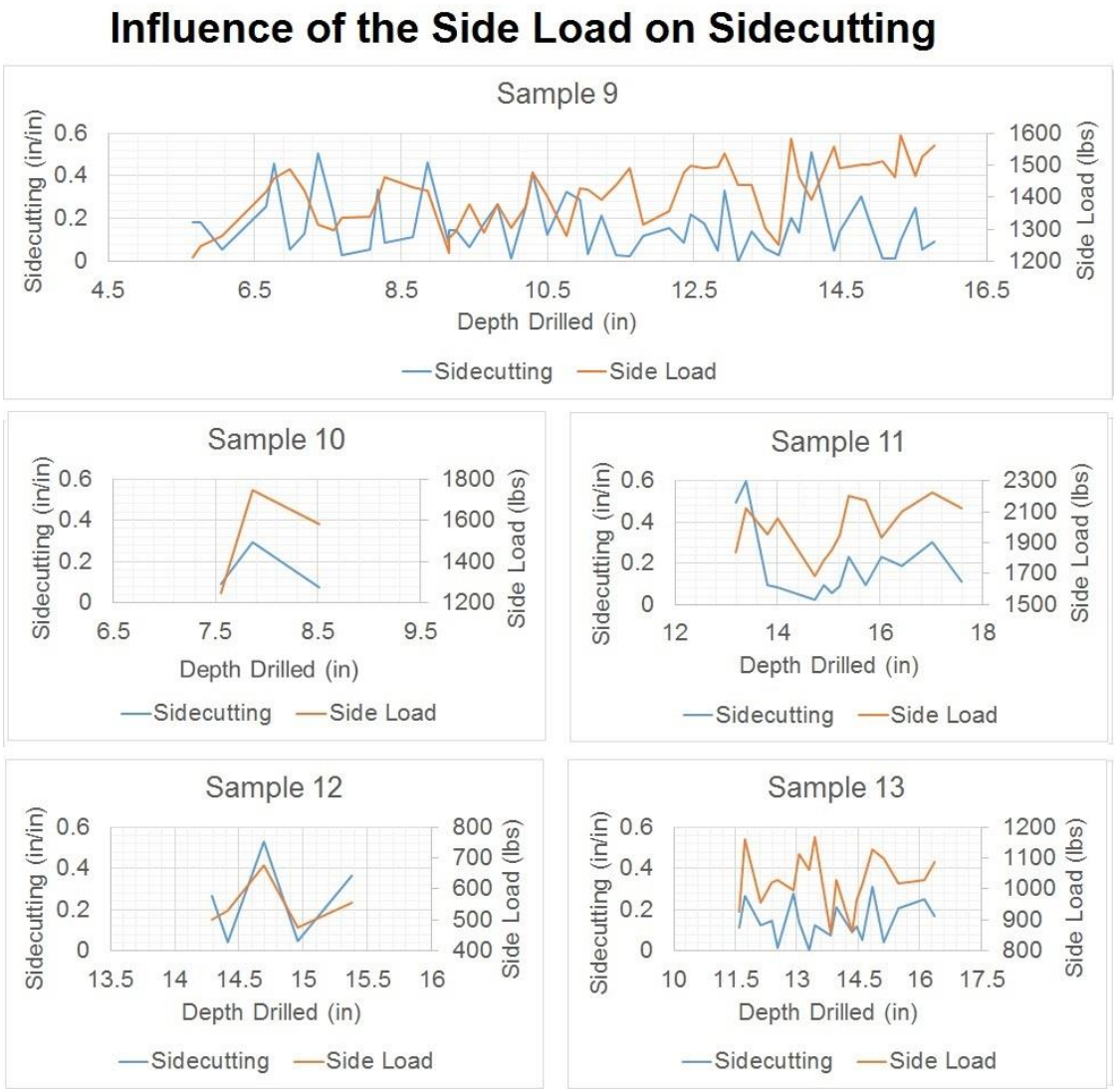

Figure 46 - Graphs showing the influence of the side load in sidecutting. It is possible to observe that the trend in sidecutting follows the trend in side load, changing accordingly.

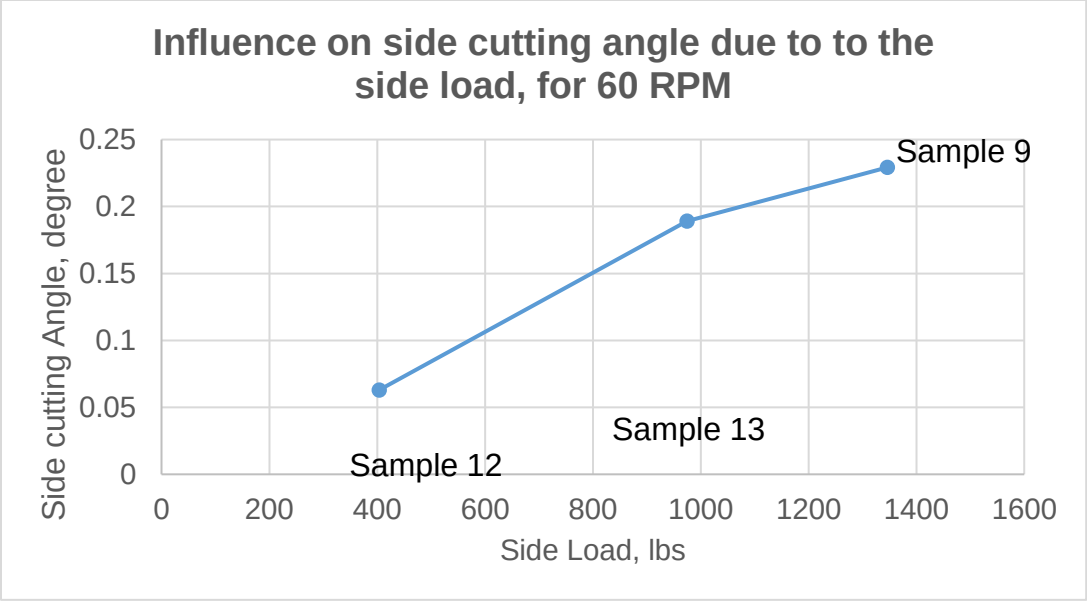

Figure 47 - Graph showing the logarithmic relationship between side load and side cutting angle. Trend matches that of Ernst, Pastusek and Lutes (2007) work in a vertical scenario.

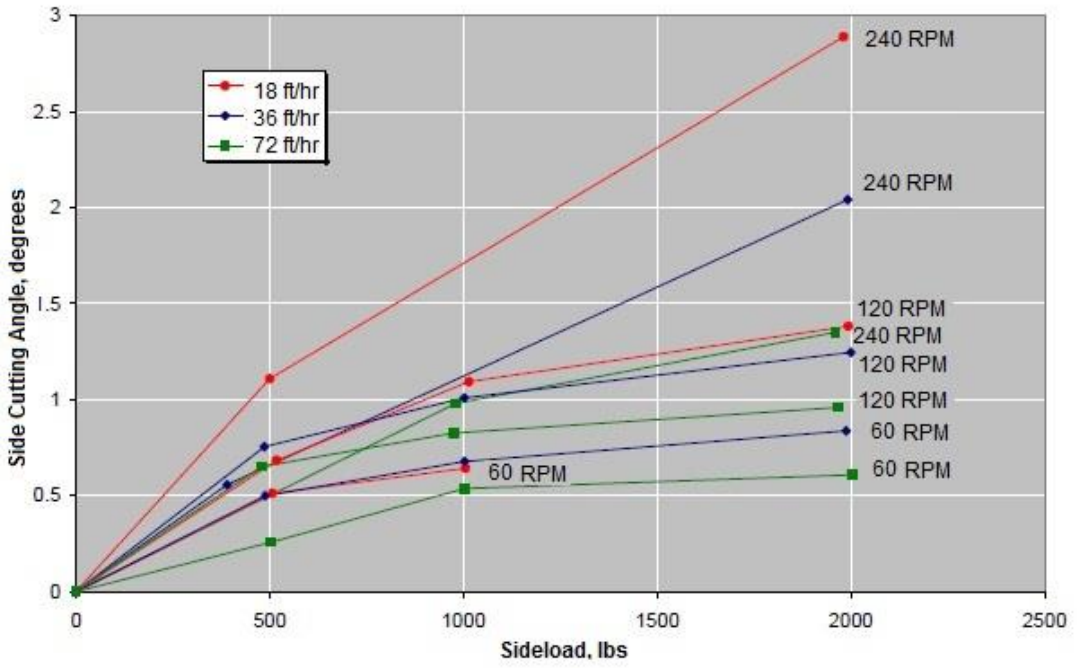

Figure 48 - Graph showing the influence of the side load on the side cutting angle for constant values of ROP and RPM on the work of Ernst, Pastusek and Lutes (2007), corroborating the conclusions reached by the present paper.

The lack of real time data for the RPM prevented graphical analysis and tracking the effects of the RPM within each sample, but a simple analysis is possible when comparing Samples 9, 10 and 11. Relative to Sample 9, Sample 10 had an increase of 50% in RPM while the average WOB and side load were maintained within 4% and 9% respectively. The result for the side cutting angle for Sample 10 presented an increase of 277% when compared to Sample 9. This occurred despite the fact that an increase of 44% was seen in ROP which can decrease the side cutting angle in some cases based on the work of Ernst, Pastusek and Lutes (2007) (the effects of ROP on the sidecutting will be further analyzed). Sample 11 had an increase of 100% on the RPM, but it saw a significant increase in side load and ROP (46% and 209%, respectively), when compared to Sample 9. The sidecutting angle increased 387% as a result.

Therefore it is easy to conclude that the RPM is a very influential parameter when controlling the steerability of a bit. This occurs because the faster you rotate the bit, more side-cuts will be done per foot, allowing for a higher steerability.

The trend observed in this work follows the same trend found in the work of Ernst, Pastusek and Lutes (2007). In the lower strength sample (6000 psi), they observed that at a constant side load (2000 lbs), doubling the RPM (from 120 to 240) would result in an increase of over 100% on the side cutting angle for 18 ft/hr, 65% for 36 ft/hr and 50% for 72 ft/hr. Samples 10 and 11 had an RPM increase of 50% and 100%, respectively, and they also had an increase of 44% and 209% on ROP. If Ernst, Pastusek and Lutes (2007) had tested a RPM of 90

at a side load of 1500 lbs, and assuming a proportional relationship, they would have increased sidecutting angle by 26.5% for a sample at 90 RPM and 1500 lbs. The increase in the sidecutting angle goes to 53% when they changed the RPM from 60 to 120. **Figure 49** shows the trend discussed. It should be noted that the lack of a linear behavior observed in the present study is due to the other parameters, such as WOB, ROP and side load not being constant.

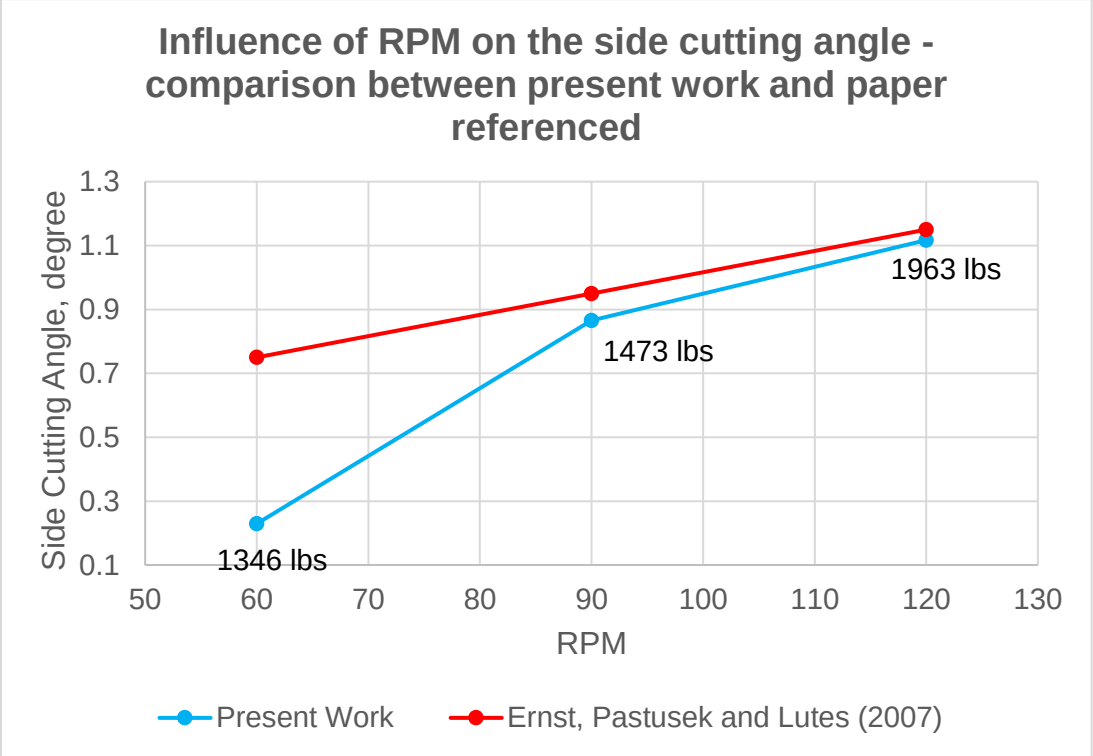

Figure 49 - Graph showing the influence of the RPM on the side cutting angle and showing the similar trend seen both in the present work and the work of Ernst, Pastusek and Lutes (2007). The lack of a linear trend on the present work is due to the non-constant values of the other parameters, especially the side load.

Ernst, Pastusek and Lutes (2007), propose in their work that the influence of WOB in steerability is due to the changes it generates in ROP. It was not possible to see the influence of WOB on the ROP of the samples due to their decreasing compressive strength with depth. Analyzing **Figure 50**, it can be seen that Samples 10, 12 and 13 had constant ROP values, even with a change in the WOB. In Samples 12 and 13, the decrease of the WOB was probably compensated by the decrease in the compressive strength of the rock with depth of the samples, maintaining the ROP constant. However Sample 10 had an increase in WOB that was not reflected on ROP. Considering that the depth analyzed for that sample is closer to the top, it is possible that the drilling was taking place in a stronger part of the sample and the increase in WOB was not sufficient to increase the ROP. The ROP in Sample 11 also did not reflect the increase in WOB towards the end of the drilling operation. Sample 9 was the only sample that presented the expected decrease in ROP with the decrease in WOB.

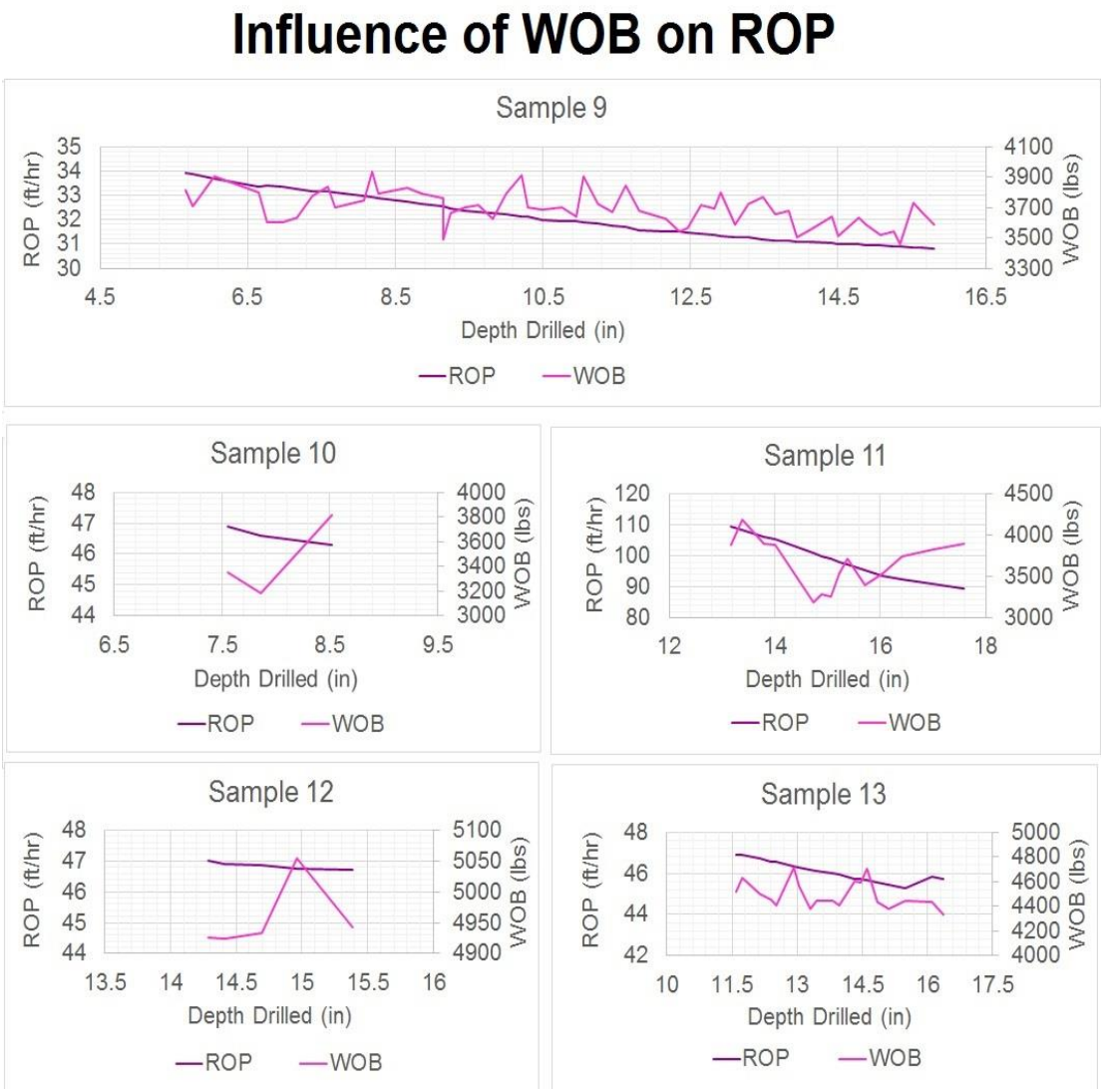

Figure 50 - Graphs showing the relationship between WOB and ROP, where it is possible to see that the only sample that had the expected decrease in ROP with a decrease in WOB was Sample 9.

Analyzing **Figure 51** for an influence of the WOB on sidecutting, it is possible to see that in Samples 9, 10 and 12, the trends are inverse and that the sidecutting is clearly following the side load trend. Samples 11 and 13, on the other hand present WOB trends very similar to the trend in side load, therefore

the fact that sidecutting is responding accordingly, and not inversely like on the other samples, is most likely not related to the changes in WOB.

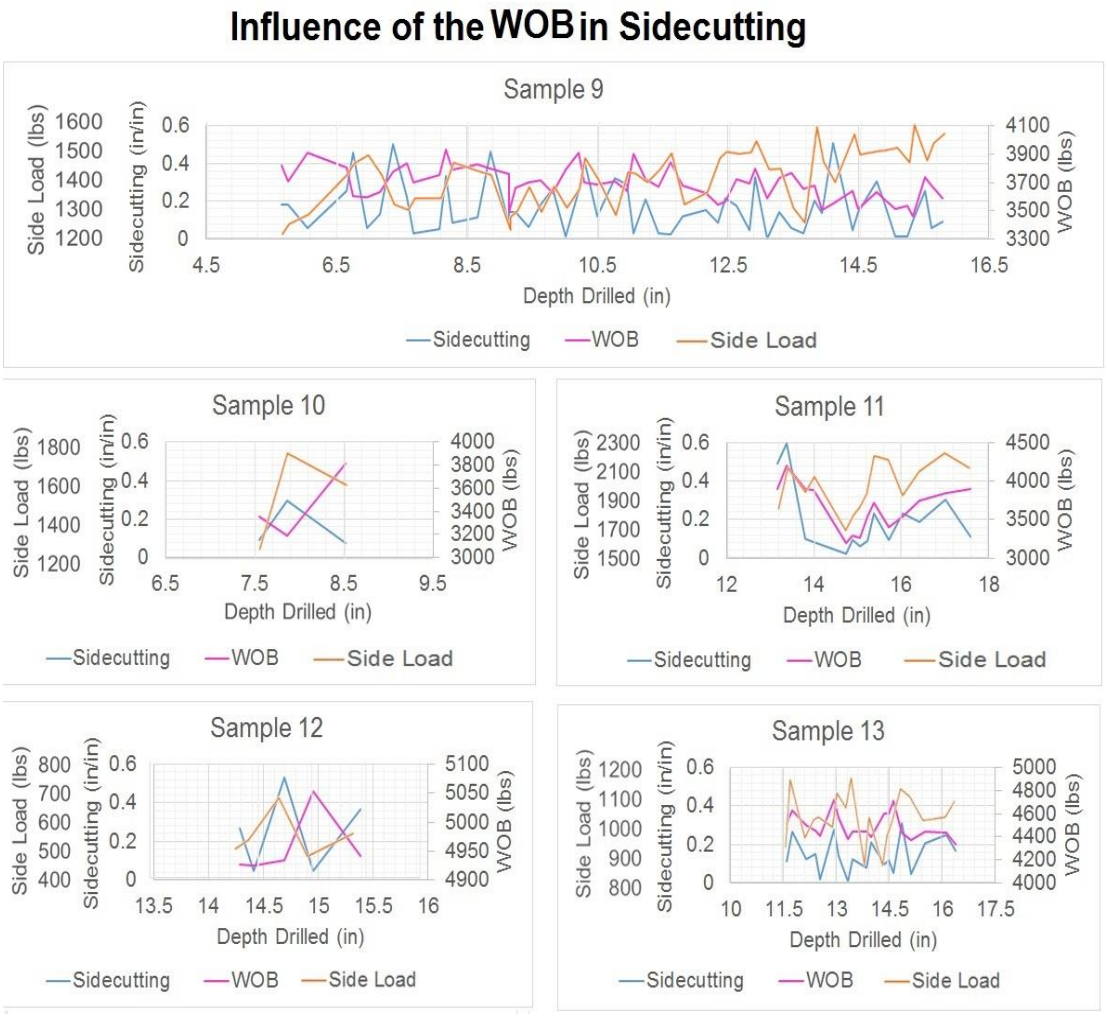

Figure 51 - Graphs showing the influence of WOB on side cutting, where it is possible to see an inverse relationship between the parameters on Samples 9, 10 and 12. Samples 11 and 13, on the other hand, present similar patterns of WOB and side load, and therefore the fact that sidecutting is responding accordingly is most likely due to side load and not WOB.

Analyzing **Figure 52** it is possible to note that all samples had an increase in ROP when compared to Sample 9. If all the other parameters were constant, it would be expected to see a decrease in sidecutting on the other samples. Sample 11 had the highest variation in ROP, a decrease of 18% during the drilling operation. Although the sidecutting value initially decreases (which can be attributed to the difficulty in controlling the side load during the drilling) it is possible to observe an increase in the sidecutting as the drilling continues. Even though the side load increases as well, this pattern of increase in sidecutting was not observed in any of the other samples, where they have a flatter tendency. Therefore it is possible that the effect of the decrease in ROP is being observed. The decrease in sidecutting was seen on Samples 12 and 13, however, both of them had a decrease in side load as well. Samples 10 and 11 also had their ROP increased, and did not respond with a decrease in sidecutting. However, the RPM and the side load were increased on those samples as well, thus making it possible to conclude that the change in RPM and side load nullified the expected effect of the ROP.

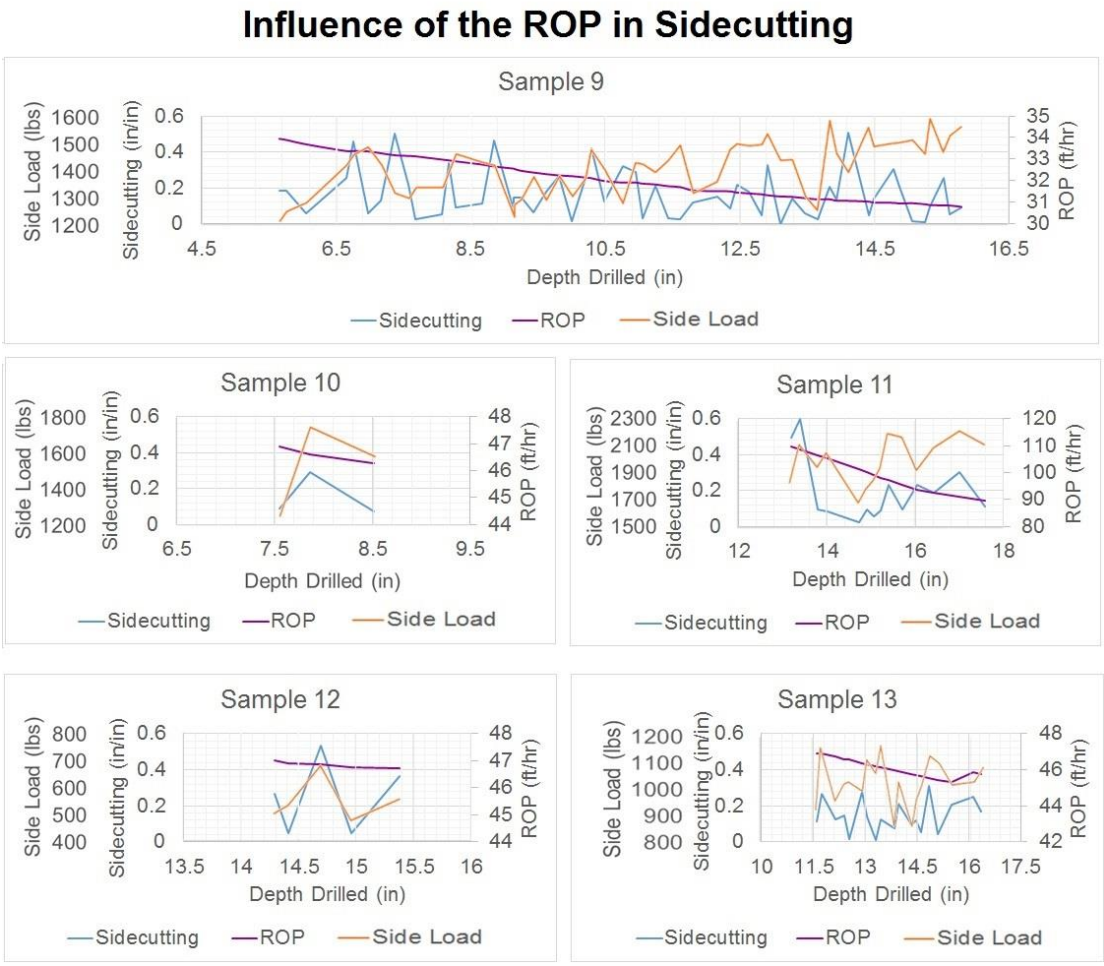

Figure 52 - Graphs showing the influence of ROP on the sidecutting, where it is possible to observe the slight increase in sidecutting in Sample 11 as it suffers the highest decrease in ROP during the drilling operations.

This conclusion is corroborated by Ernst, Pastusek and Lutes (2007), where they show that the effects of ROP are more significant at higher RPM. **Figure 53** shows that the slopes tend to flatten with the decrease in RPM.

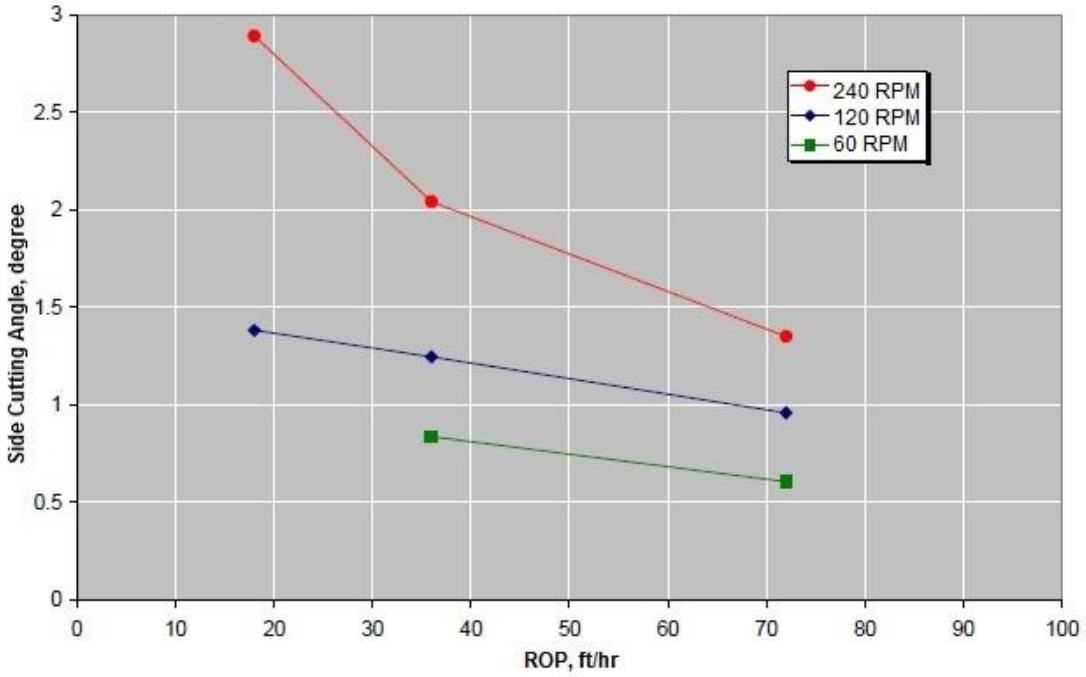

Figure 53 - Graph showing the influence of ROP on sidecutting angle at different RPMs found by Ernst, Pastusek and Lutes (2007), where it is possible to observe that the effect of ROP tends to decrease with the decrease of RPM.

MSE is a measure of the efficiency of the drilling operation, however, this efficiency is only taken into account as in forward drilling. Thus when steering the bit that measurement is assumed to show some inefficiency. The test rig was designed to minimize bit dysfunction which in turn minimizes MSE. Comparing to Sample 9, all samples had the average value of the MSE decreased but Sample 10 (2%increase), which can be explained by the increase of 9% in side load. Sample 11 was expected to have a higher MSE value, due to the fact that this samples had the highest side load. However, it presented the lowest average value (decreasing 40% when compared to Sample 9), which can be explained by

the increase of 209% in ROP. Samples 12 and 13 both had their side loads decreased, and their MSE values followed.

Analyzing **Figure 54**, it is possible to see a relationship between WOB, side load and MSE. On Sample 9 and 11 it is possible to see that the MSE trend is following the side load trend proportionally, which is expected, considering that an increase in side load would disturb the system and make the drilling less efficient, increasing the MSE. This behavior was also observed on the last couple of inches of drilling for Sample 13. Sample 12 and the beginning of Sample 13 presented a MSE behavior inverse to WOB, this pattern is a common diagnostic in situations where whirl is occurring. Increasing WOB effectively stabilizes the bit in the rock creating a more efficient drilling process and reducing MSE.

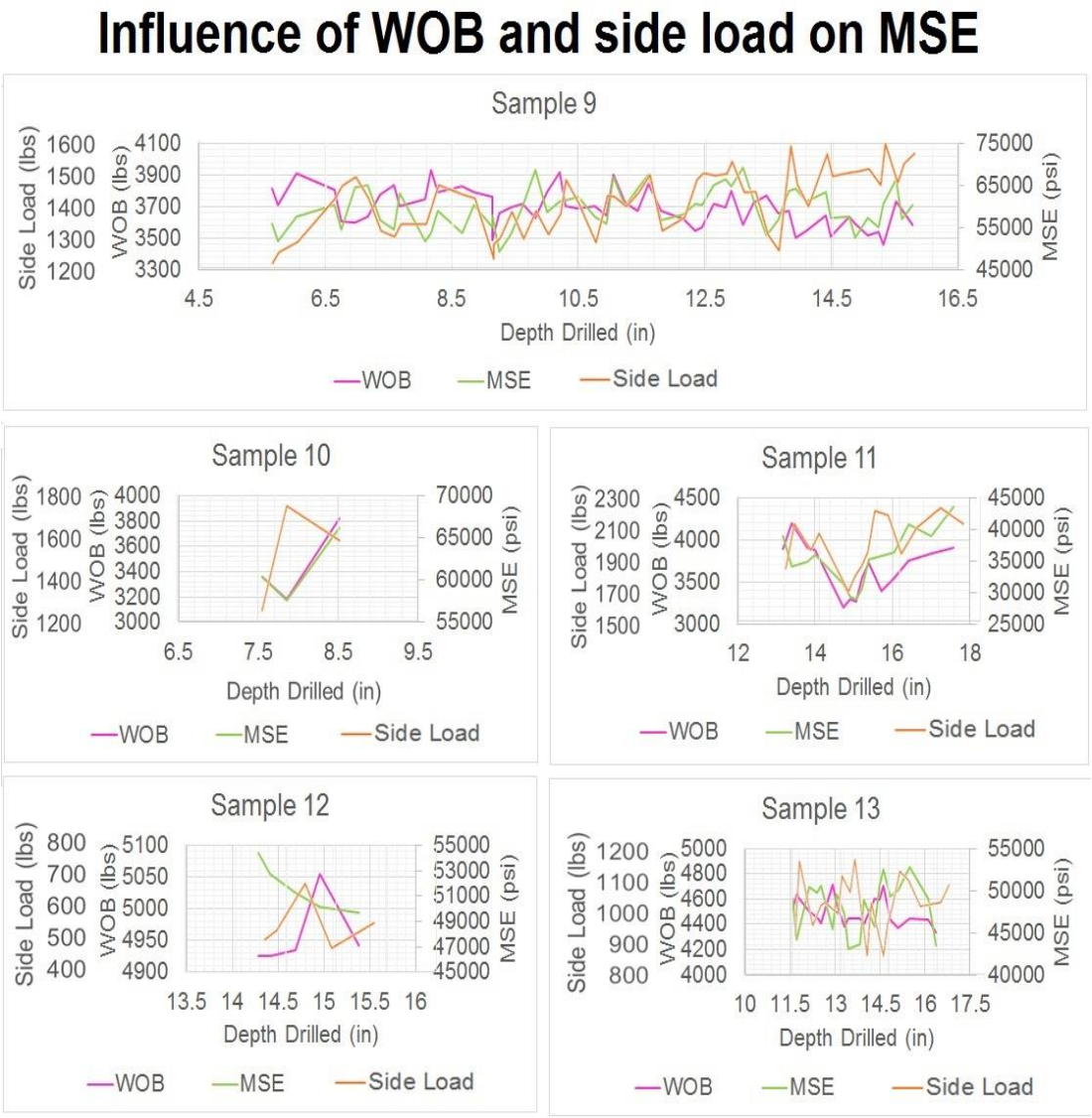

Figure 54 - Graphs showing the relationship between WOB, side load and MSE, where it is possible to see a proportional relationship between side load and MSE for Samples 9 and 11, and an inverse relationship between WOB and MSE for Samples 12 and 13, indicating the presence of whirl.

An inspection of the bottom hole pattern (**Figure 55**) shows a spiral wellbore pattern with randomly spaced periods. The pattern period is determined by the distance between spiral marks on the sample. The measurements ranged from 2.5 in between the first two, then 1.0 in, 1.5 in, 1.0 in, 2.0 in to 1.0 in. While lack

of data makes this pure speculation, the pattern does suggest a coupled whirl and side load phenomenon. The changing in pattern period could be due to the lack of control of the parameters during the drilling operations which could change the pattern significantly. This type of pattern was observed only on one side of more than one sample, with Sample 6 being the one with the most distinguished effect. However, there is not enough data to prove/disprove this theory and considering that the picture was taken a couple of months after the drilling, it could be explained by dust deposit, effects of weathering on the samples or even just the side loads variations during the drilling operations.

Figure 55 - Bottom hole pattern of Sample 6, showing a pattern that could indicate whirl during the drilling operations.

The present work tried to replicate the findings of Ernst, Pastusek and Lutes (2007) on a horizontal set up. The test rigs had some differences regarding the set up of the experiments. The present work took the experiments to a horizontal set up, the hydraulic system pushed the sample into the bit (and not the other way around like on a normal drilling operation and the mentioned work), the side load system applied the force into the sample carriage and not directly on the bit and it was used a manual control for WOB and side load, which made it harder to maintain constant values for those parameters. In addition, the samples used on the present work had a variation in compressive strength with depth. However,

it is important to note that despite the differences in the experiments, most of the relationships between drilling parameters and sidecutting observed were the same.

Both works presented a logarithmic relationship between RPM and side load when influencing the sidecutting angle. However, the effect of varying ROP was not observed in the present work. Ernst, Pastusek and Lutes (2007) were able to observe higher sidecutting angle for lower ROP when other parameters were held constant. In terms of coupled effects, they also observed instances where higher RPM and ROP would have steerability equivalence to a lower RPM and ROP.

The similarities between both studies lead to the conclusion that when trying to increase/decrease sidecutting angle in a horizontal well, the bit will respond to the change in drilling parameter in a similar manner than in a vertical well.

5 CONCLUSION AND FUTURE WORK

5.1 Conclusion

Based on the theoretical and experiment work present through the course of this thesis, it is possible to conclude that:

- It was possible to see a direct relationship between side load and sidecutting angle, with the latter increasing, with the increase in the former
- RPM proved to have a significant influence on the sidecutting angle, with a logarithmic relationship with the side load, which was same relationship observed by Ernst, Pastusek and Lutes (2007)
- The influence of WOB on ROP was only observed in Sample 9 and was not clear on the rest of the samples, possibly due to the change in compressive strength with depth on the samples
- The ROP influence on sidecutting was only observed in Sample 11 and was not able to be identified comparing the samples due to the fact that RPM and side load changed as well, and their effect ended up overshadowing the effect of the ROP
- The trend observed on the MSE was opposite to the side load, which is consistent to the fact that MSE measures the efficiency of the drilling operation, and applying a side load is basically disturbing the bit, However, Sample 11 presented a behavior contrary to what is known about drilling efficiency and dysfunctions such as whirl, where increasing side load caused a decrease in MSE. The reason for this is unknown and needs to

be further investigated as it does not represent common engineering knowledge.

- A possible pattern of coupled whirl and side load occurred, as suggested by the inverse relationship between WOB and MSE on Samples 12 and 13 and the bottom hole patterns
- Considering that the relationships observed on the present work matched the ones observed by Ernst, Pastusek and Lutes (2007), it was possible to conclude that when trying to increase/decrease sidecutting angle in a horizontal well, the bit will respond to the change in drilling parameter in a similar manner than in a vertical well.

5.2 Future Work

For future work it is recommended that further adjustments to the rig be made. One of the biggest limiters for operating the rig was the weather. The rig is located outdoors due to its size, and it is exposed to weather conditions. In addition, dealing with sensitive and electrical equipment prevent operations during rain. While the ideal instruments for the rig, the originally installed rod sensors are extremely sensitive to heat, preventing its use when exposed to weather variations. A controllable lab environment would be ideal but in the event it is not possible, improved sensors would be recommended. Furthermore, the drilling operation had to be manually controlled, through valves and switches, generating variable values throughout the drilling process. Automated systems to control the

WOB and side load that could be set in the beginning of the drilling operations and maintained constant, would enable a more uniform analysis. The real-time value for RPM is still not set up and it would be useful to have that control as well. In addition the hydraulic and side load motors should be redesign so it will not be a limiter during further operations.

The samples used on the present work were made from a concrete recipe and the curing method was proved inefficient, thus the variation in compressive strength throughout the sample. It is suggested that during the pouring of the samples, compression be applied, in order to prevent entrapped air. Also a better method of keeping the samples moist during the 28 day requirement is suggested. It would be interesting to have cores from real formations and compare the behavior of the bit with the one from a concrete sample with similar compressive strength, as well as using a wider range of compressive strengths to see how the bit would behave in harder formations.

In addition, more drilling tests should be done varying the WOB, ROP, RPM and side load to have a more complete matrix. Using different bit configurations is also a good way to see how the bit profile influence on steerabilty and what combinations of the parameters work better for each bit profile, turning the directional drilling process more efficient.

REFERENCES

Boualleg, R., Sellami, H., Menand, S. and Simon, C. 2006. Effect of Formation Anisotropy on Directional Tendencies of Drilling Systems. Presented at the IADC/SPE Drilling Conference, Miami, Florida, USA, 21-23 February. SPE-98865-MS. http://dx.doi.org/10.2118/98865-MS.

Boualleg, R., Sellami, H., Rouabhi, A., Menand, S. and Simon, C. 2007. Effect of Rocks Anisotropy on Deviation Tendencies of Drilling Systems. Presented at the 11th Congress of the International Society for Rock Mechanics, Lisbon, Portugal, 9-13 July.

Cheatham Jr., J. B. and Ho, C. Y. 1981. A Theoretical Model for Directional Drilling Tendency of a Drill Bit in Anisotropic Rock. Society of Petroleum Engineers, SPE-10642-MS.

Dupriest, F. E., Elks Jr., W. C., S., O., Pastusek, P. and Zook, J. R. 2010. Borehole-Quality Design and Practices To Maximize Drill-Rate Performance. Presented at the SPE Annual Technical Conference and Exhibition, Florence, Tuscany, Italy, 20-22 September. SPE-134580-PA. http://dx.doi.org/10.2118/134580-PA.

Ernst, S., Pastusek, P. and Lutes, P. 2007. Effects of RPM and ROP on PDC Steerability. Presented at the IADC/SPE Drilling Conference, Amsterdam, The Netherlands, 20-22 February. SPE-105594-MS. http://dx.doi.org/10.2118/105594-MS.

Gerbaud, L., Menand, S. and Sellami, H. 2006. PDC Bits: All Comes From the Cutter/Rock Interaction. Presented at the IADC/SPE Drilling Conference, Miami, Florida, USA, 27-30 September. SPE-98988-MS. http://dx.doi.org/10.2118/98988-MS.

Hibbeler, R. C. 2013. *Mechanics of Materials*, 9th edition. New Jersey, New York: Prentice Hall (Reprint).

Inglis, T. A. 1987. *Petroleum Engineering and Development Studies, Volume 2 - Directional Drilling*, first edition edition. Norwell, MA: Graham & Trotman (Reprint).

Jogi, P. N., Burgess, T. M. and Bowling, J. P. 1986. Predicting the Build/Drop Tendency of Rotary Drilling Assemblies. Presented at the IADC/SPE Drilling Conference, Dallas, Texas, USA, 10-12 February. SPE-14768-PA. http://dx.doi.org/10.2118/14768-PA.

Jones, S., Sugiura, J. and Barton, S. 2008. Results from Systematic Rotary-Steerable Testing with PDC Drill-Bits Depict the Optimal Balance Between Stability, Steerability and Borehole Quality. Presented at the IADC/SPE Drilling Conference, Orlando, Florida, USA, 4-6 March. SPE-112579-MS. http://dx.doi.org/10.2118/112579-MS.

Kakogianis, S. and Schroder, G. 2011. Applications. *Wikispaces - Directional Drilling Well Design and Equipment*. 11 May 2011, https://drilleng-group4-directionaldrilling-1.wikispaces.com/Applications (accessed April 14 2016).

Lubinski, A. and Woods, H. B. 1953. Factors Affecting the Angle of Inclination adn Dog-Legging in Rotary Bore Holes. Presented at the Spring Meeting of the Mid-Continent District, Division of Production, Tulsa, Oklahoma, USA, March. API-53-222.

Menand, S., Sellami, H. and Simon, C. 2003. PDC Bit Classification According to Steerability. Presented at the SPE/IADC Drilling Conference, Amsterdam, Netherlands, 16-19 February. SPE-79795-MS. http://dx.doi.org/10.2118/79795-MS.

Menand, S., Sellami, H., Simon, C., Besson, A. and Da Silva, N. 2002. How Bit Profile and Gauges Affect Well Trajectory. Presented at the IADC/SPE Drilling Conference, Dallas, Texas, USA, 26-28 February. SPE-74459-MS. http://dx.doi.org/10.2118/74459-MS.

Menand, S., Simon, C., Gaombalet, J., Macresy, L., Ben Hamida, M., Amghar, Y., Denoix, H., Cuiller, B. and Sinardet, H. 2012. PDC Bit Steerability Modeling and Testing for Push-the-bit and Point-the-bit RSS. Presented at the IADC/SPE Drilling Conference and Exhibition, San Diego, California, USA, 6-8 March. SPE-151283-MS. http://dx.doi.org/10.2118/151283-MS.

Millheim, K. 1977. The Effect of Hole Curvature on the Trajectory of a Borehole. Presented at the 52nd Annual Fall Technical Conference and Exhibition of the Society of Petroleum Engineers of AIME, Denver, Colorado, USA, 9-12 October. SPE-6779-MS. http://dx.doi.org/10.2118/6779-MS.

Millheim, K. 1982. Computer Simulation of the Direcional Drilling Process. Presented at the International Petroleum Exhibition and Technical Synposium of the Society of Petroleum Engineers, Bejing, China, 18-26 March. SPE-9990-MS. http://dx.doi.org/10.2118/9990-MS.

Millheim, K., Gubler, F. H. and Zaremba, H. B. 1978. Evaluating and Planning Directional Wells Utilizing Post Analysis Techniques and Three Dimensional Bottom Hole Assembly Program. Presented at the European Offshore Petroleum Conference and Exhibition, London, England, 24-27 October. SPE-8079-MS. http://dx.doi.org/10.2118/8079-MS.

Millheim, K. and Warren, T. 1978. Side Cutting Characteristics of Rock Bits and Stabilizers While Drilling. Presented at the 53rd Annual Technical Conference and Exhibition of the Society of Petroleum Engineers of AIME, Houston, Texas, USA, 1-3 October. SPE-7518-MS. http://dx.doi.org/10.2118/7518-MS.

Mitchell, R. F. and Miska, S. Z. 2010. *Fundamentals of Drilling Engineering*. USA: Society of Petroleum Engineering (Reprint).

Pastusek, P., Brackin, V. and Lutes, P. 2005. A Fundamental Model for Prediction of Hole Curvature and Build Rates With Steerable Bottomhole Assemblies. Presented at the SPE Annual Techinical Conference and Exhibition, Dallas, Texas, USA, 9-12 October. SPE-95546-MS. http://dx.doi.org/10.2118/95546-MS.

Tingey, D. 2015. *Design, Fabrication and Preliminary Testing of Experimental Rock Drilling Rig*. MS Thesis, Texas A&M University, College Station, Texas, USA (August 2015).

Walker, B. H. 1986. Factors Controlling Hole Angle and Direction. *Journal of Petroleum Technology* **38** (11): 1,171 - 1,173. SPE-15963-PA. http://dx.doi.org/10.2118/15963-PA.

Wilson, J. K. 2013. Design and Analysis of a Test Rig for Modeling the Bit/Formation Interface in Petroleum Drilling Applications. MS Thesis, Texas A&M University, College Station, Texas, USA (May 2013).